

Electronic Supplementary Information

**A novel family of AIE-active *meso*-2-ketopyrrolylBODIPYs:
Bright solid-state red fluorescence, morphological properties and
application as viscosimeters in live cells**

Changjiang Yu,^{†acd} Zhenlong Huang,^{†b} Wei Gu,^a Qinghua Wu,^a Erhong Hao,*^a Yi Xiao,*^b Lijuan Jiao*^a and Wai-Yeung Wong*^c

^a The Key Laboratory of Functional Molecular Solids, Ministry of Education; School of Chemistry and Materials Science, Anhui Normal University, Wuhu 241000, China.

^b State Key Laboratory of Fine Chemicals, Dalian University of Technology, 2 Linggong Road, Dalian 116024, China.

^c Department of Applied Biology and Chemical Technology, The Hong Kong Polytechnic University, Hung Hom, Hong Kong, China.

^d State Key Laboratory of Coordination Chemistry, Nanjing University, Nanjing 210093, China.

[†] equal contribution

*To whom correspondence should be addressed. E-mail: haoehong@ahnu.edu.cn; xiaoyi@dlut.edu.cn; jiao421@ahnu.edu.cn; wai-yeung.wong@polyu.edu.hk

Contents:

1. Crystal packings and selected parameters.....	S2
2. Photophysical properties.....	S7
3. Aggregation-induced emission properties.....	S14
4. SEM and TEM images.....	S18
5. Dynamic light scattering.....	S19
6. Viscosity sensitivity studies.....	S21
7. Cell culture.....	S24
8. MTT Assay.....	S27
9. Viscosity determination in real-time during apoptosis.....	S28
10. NMR for <i>meso</i> -2-ketopyrrolyl BODIPYs.....	S29
11. HRMS for <i>meso</i> -2-ketopyrrolyl BODIPYs.....	S33
12. DFT calculations.....	S35

1. Crystal diagrams and selected data

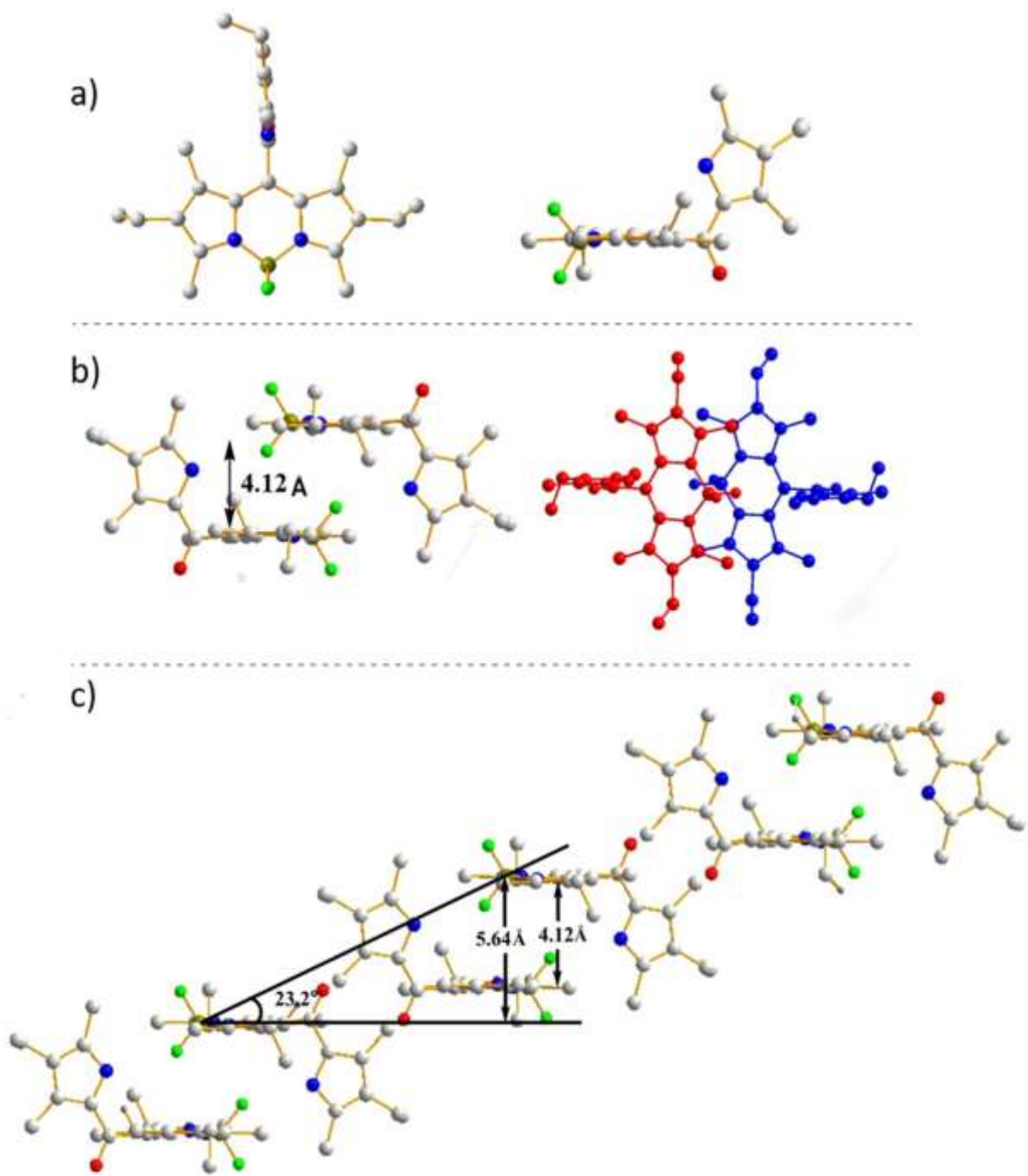


Figure S1. Crystal-packing pattern of **1a** between the adjacent interlayered crystals from side view. Interlayer distance is 4.12 \AA and tilt angle is 23.2° for coplanar inclined arrangements of its transition dipole. C, light gray; N, blue; B, dark yellow; F, green; O, red; H atoms are omitted for clarity.

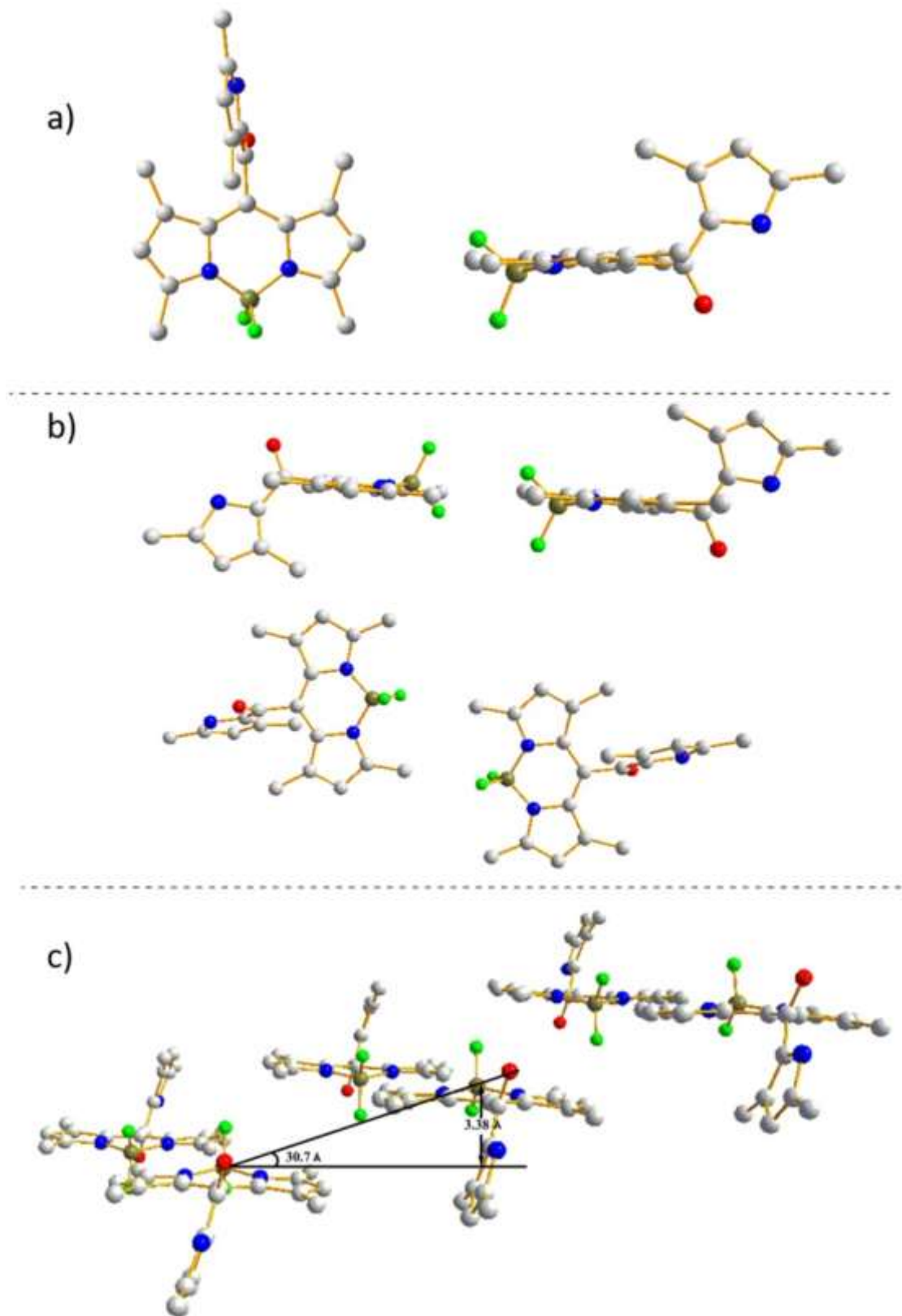


Figure S2. Crystal-packing pattern of **1b** between the adjacent interlayered crystals from side view. Interlayer distance is 3.38 Å and tilt angle is 30.7° for coplanar inclined arrangements of its transition dipole. C, light gray; N, blue; B, dark yellow; F, green; O, red; H atoms are omitted for clarity.

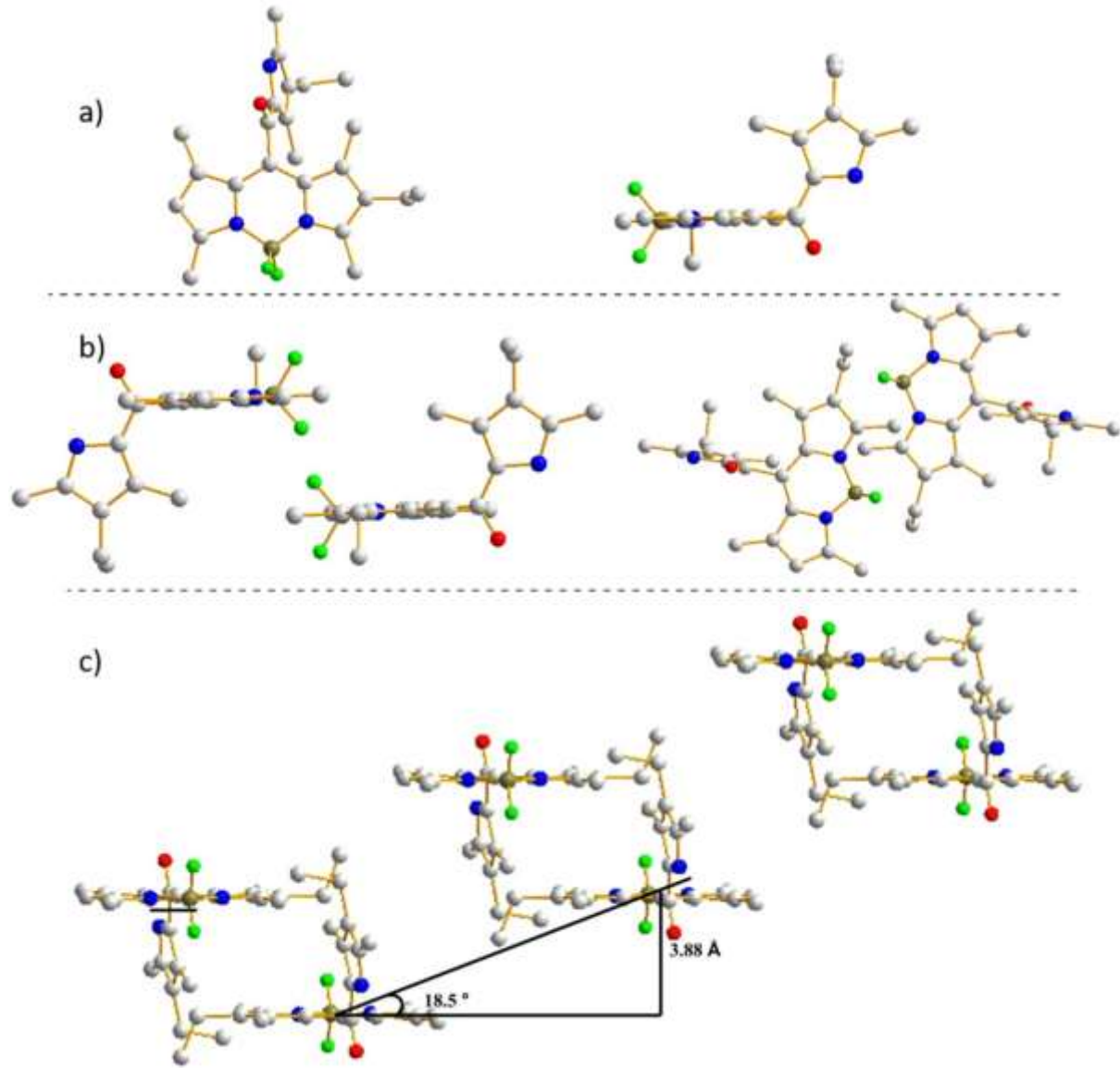
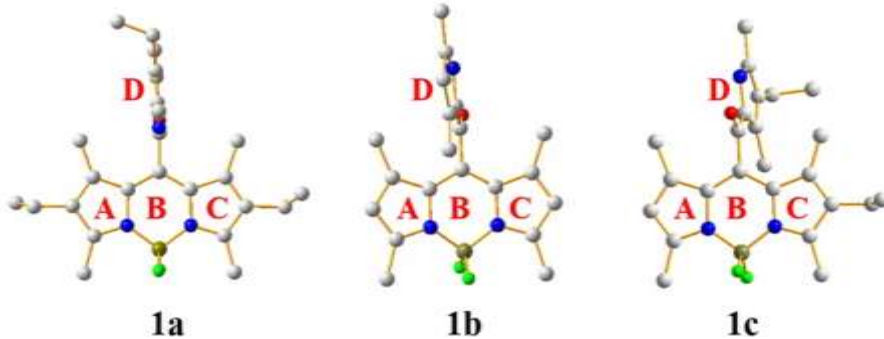


Figure S3. Crystal-packing pattern of **1c** between the adjacent interlayered crystals from side view. Interlayer distance is 3.88 \AA and tilt angle is 18.5° for coplanar inclined arrangements of its transition dipole. C, light gray; N, blue; B, dark yellow; F, green; O, red; H atoms are omitted for clarity.

Table S1. Selected bond lengths [Å] and dihedral angles [deg] of *meso*-2-ketopyrrolyl-BODIPYs **1a-c** obtained from X-ray crystallography.



	1a	1b	1c
the B-F bond distances (Å)	1.390 1.392	1.377 1.383	1.381 1.389
the B-N bond distances (Å)	1.536 1.536	1.549 1.550	1.533 1.547
dihedral angles of two coordinated pyrrolic rings A and C (deg)	5.0(2)	8.78(2)	1.51(1)
dihedral angles between the six-membered ring B composed of NBN and the BODIPY core (deg)	0.53(1)	0.61(2)	0.40(2)
dihedral angles between the <i>meso</i> -uncoordinated pyrrolic ring D and the BODIPY core (deg)	88.8(2)	72.9(1)	81.4(1)
intramolecular C-H···F hydrogen bond distances (Å)	2.602, 2.611, 2.680, 2.759	2.542, 2.728, 2.726, 2.878	2.571, 2.600, 2.707, 2.772
intermolecular C-H···F hydrogen bond distances (Å)		2.695, 2.695, 2.827, 2.827	2.578, 2.612
intermolecular N-H···F hydrogen bond distances (Å)	2.075, 2.075		

Table S2. Crystal data collection parameters for *meso*-2-ketopyrrolyl BODIPYs **1a**, **1b** and **1c** obtained from X-ray crystallography.

	1a	1b	1c
CCDC no.	1541729	1541728	1901461
formula	C ₂₆ H ₃₄ BF ₂ N ₃ O	C ₂₀ H ₂₂ BF ₂ N ₃ O	C ₂₄ H ₃₀ BF ₂ N ₃ O
M	453.37	369.22	425.32
T (K)	293(2)	293(2)	293(2)
λ (Å)	0.71073	0.71073	0.71073
crystal system	Monoclinic	Monoclinic	Monoclinic
space group	C2/c	C2/c	C2/c
a (Å)	26.649(3)	12.8894(18)	23.744(3)
b (Å)	9.8463(10)	9.0135(12)	12.2488(12)
c (Å)	19.4482(19)	31.806(4)	19.0154(18)
α (deg)	90	90	90
β (deg)	101.3930(10)	93.146(2)	101.276(2)
γ (deg)	90	90	90
V (Å ³)	5002.5(9)	3689.6(9)	5423.7(10)
Z	8	8	8
D _{calcd} (mg m ⁻³)	1.204	1.329	1.042
μ mm ⁻¹	0.083	0.096	0.073
F(000)	1936	1552	1808.0
θ range (deg)	1.56 - 27.63	2.76 - 27.62	1.249 to 24.996
reflections collected/ unique	21129 / 5791	15525 / 4277	18895 / 4776
R (int)	0.0294	0.0222	0.0339
goodness-of-fit on F ²	1.058	1.047	1.094
R1, wR2 [I>2σ(I)]	0.0637, 0.2012	0.0458, 0.1300	0.0544, 0.1846
R1, wR2 (all data)	0.1044, 0.2386	0.0618, 0.1441	0.0718, 0.1948
Largest diff. peak and hole, e. Å ⁻³	0.306, -0.240	0.277, -0.210	0.21, -0.17

2. Photophysical properties

Table S3. Photophysical properties of *meso*-2-ketopyrrolyl BODIPYs **1a** and **1b** in several organic solvents and powder state.

dyes	solvents	$\lambda_{\text{abs}}^{\text{max}}$ (nm)	$\lambda_{\text{em}}^{\text{max}}$ (nm)	$\log \epsilon_{\text{max}}^{\text{a}}$	ϕ^{b}	Stokes shift (cm ⁻¹)
1a	cyclohexane	532	557	4.89	0.12	844
	toluene	534	561	4.84	0.19	901
	dichloromethane	534	560	4.81	0.21	869
	tetrahydrofuran	530	554	4.84	0.18	817
	acetonitrile	529	555	4.79	0.10	886
	methanol	530	549	4.80	0.13	653
	glycerol	534	554	4.82	0.43	676
	solid state	-	661	-	0.13	-
1b	cyclohexane	508	534	4.91	0.12	958
	toluene	510	537	4.91	0.07	986
	dichloromethane	509	533	4.90	0.08	885
	tetrahydrofuran	507	530	4.93	0.05	856
	acetonitrile	504	526	4.88	0.03	830
	methanol	506	522	4.86	0.06	606
	glycerol	510	526	4.89	0.15	596
	solid state	-	620	-	0.21	-
1c	cyclohexane	520	548	4.88	0.03	983
	toluene	522	549	4.86	0.08	942
	dichloromethane	521	548	4.83	0.10	946
	tetrahydrofuran	518	544	4.80	0.03	923
	acetonitrile	517	543	4.78	0.01	926
	solid state	-	653	-	0.25	-
1d	cyclohexane	519	547	4.87	0.03	986
	toluene	522	549	4.84	0.08	942
	dichloromethane	521	548	4.80	0.10	946
	tetrahydrofuran	518	543	4.81	0.03	889
	acetonitrile	517	541	4.79	0.01	858
	solid state	-	644	-	0.22	-

^aMolar absorption coefficients of **1a-d** are calculated at the maximum of the highest peak in their absorption spectra. ^bFluorescence quantum yields (ϕ) of **1a-d** were evaluated by using integrating sphere in the above solvents (excited at 480 nm for **1b-d** in the above solvents, excited at 500 nm for **1a**) and powder state (excited at 550 nm for **1a** and 500 nm for **1b-d**). The standard errors are less than 5%.

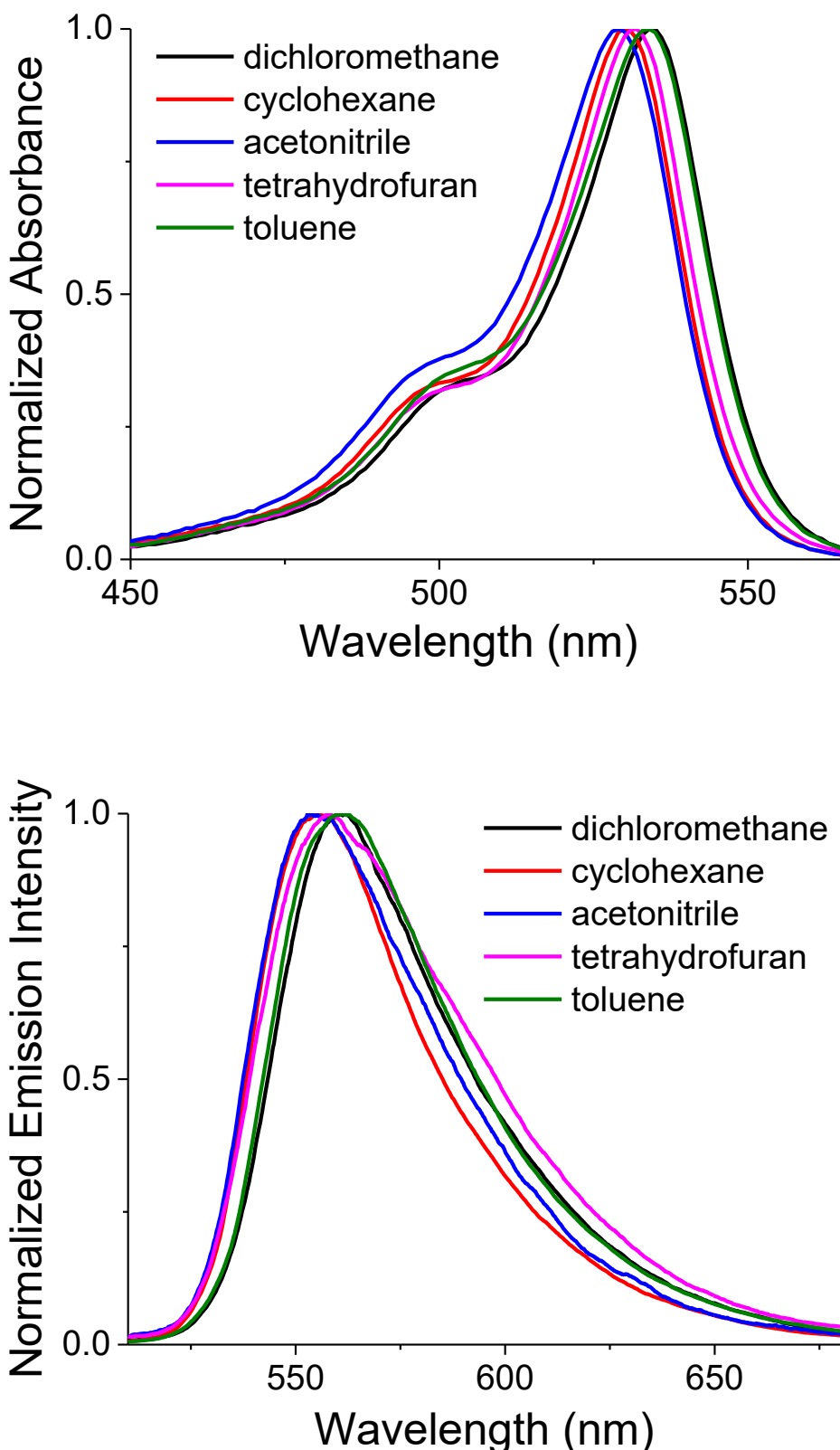


Figure S4. Normalized UV-vis (top) and fluorescence spectra (bottom) of **1a** (5 μM) in different solvents, excited at 500 nm.

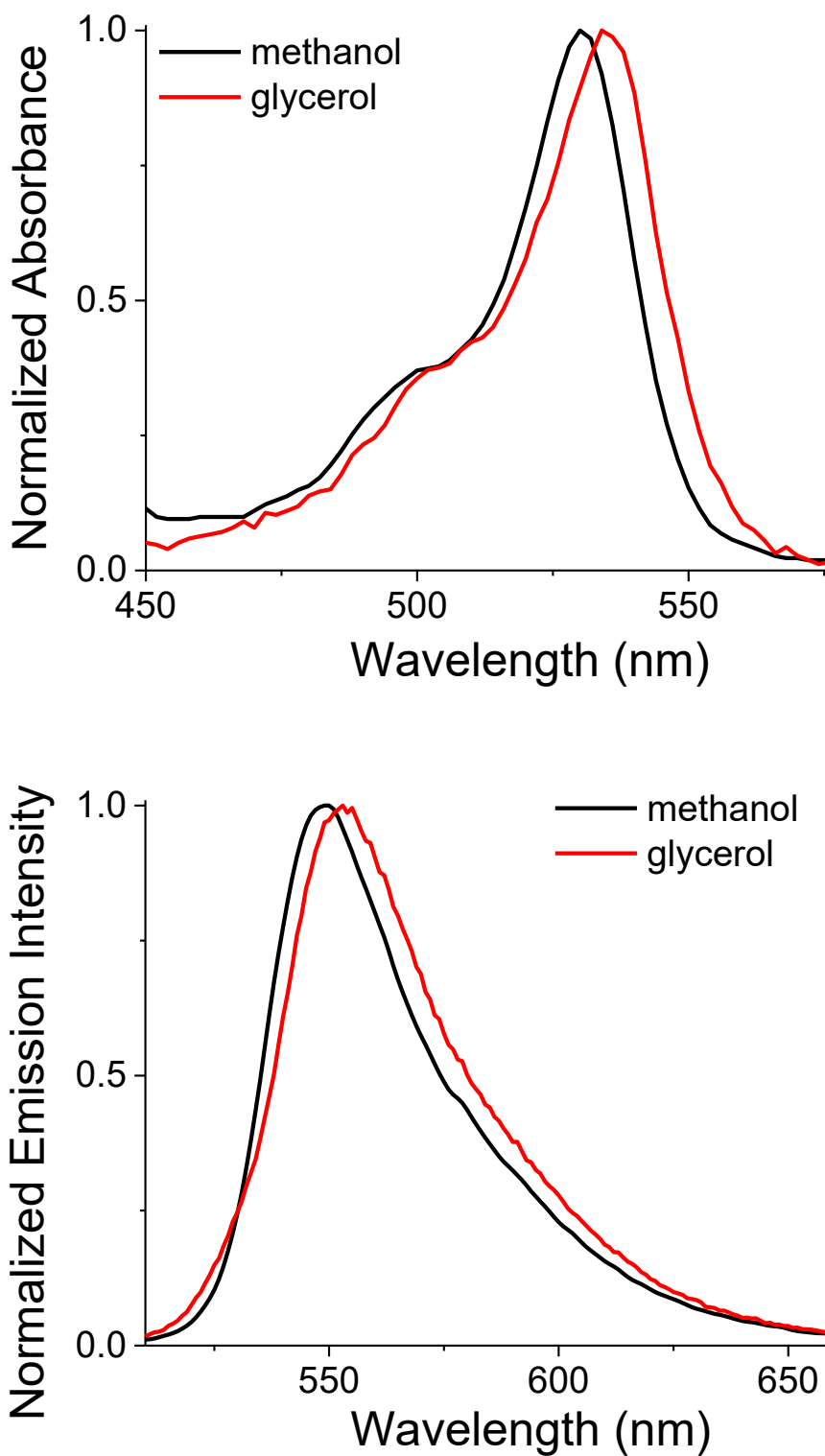


Figure S5. Normalized UV-vis (top) and fluorescence spectra (bottom) of **1a** (5 μ M) in methanol and glycerol, excited at 500 nm.

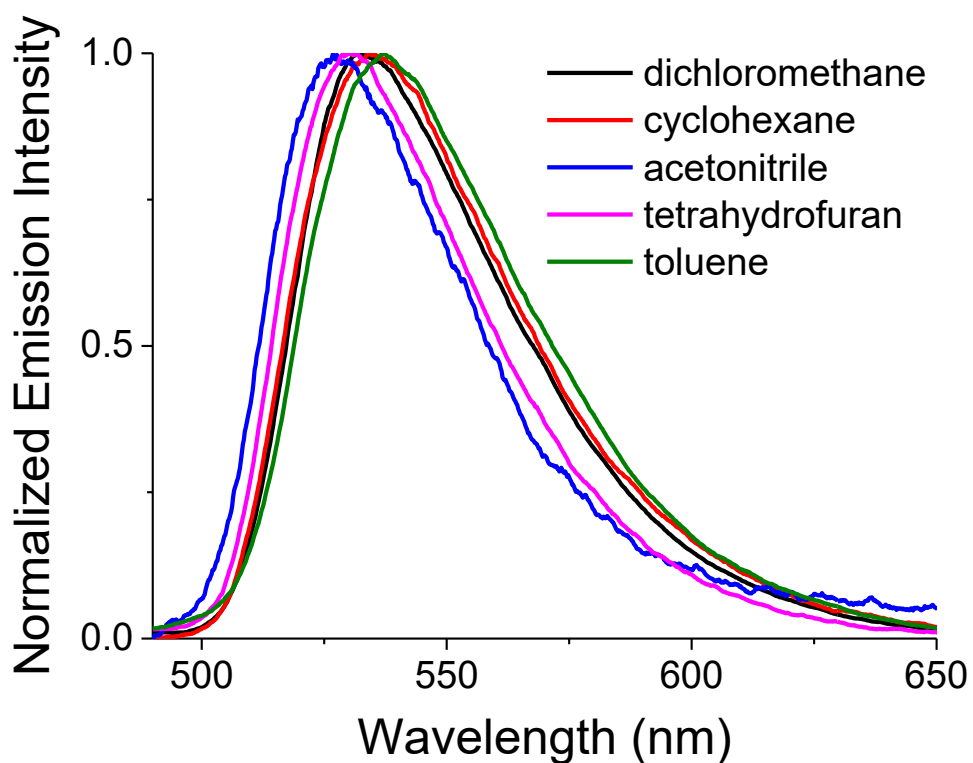
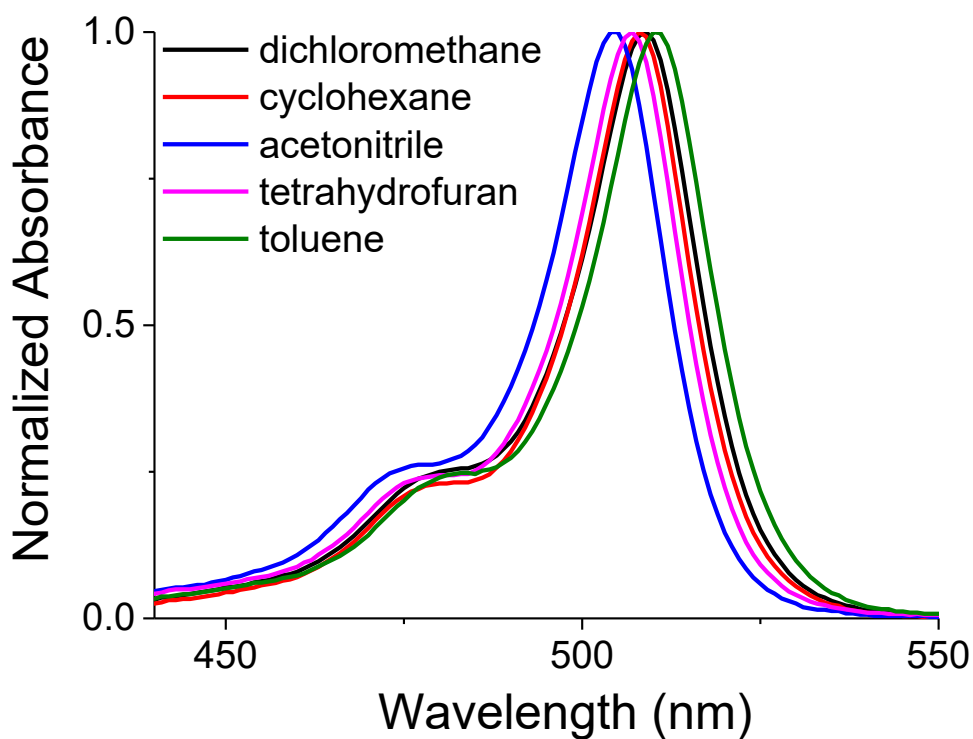


Figure S6. Normalized UV-vis (top) and fluorescence spectra (bottom) of **1b** (5 μM) in different solvents, excited at 480 nm.

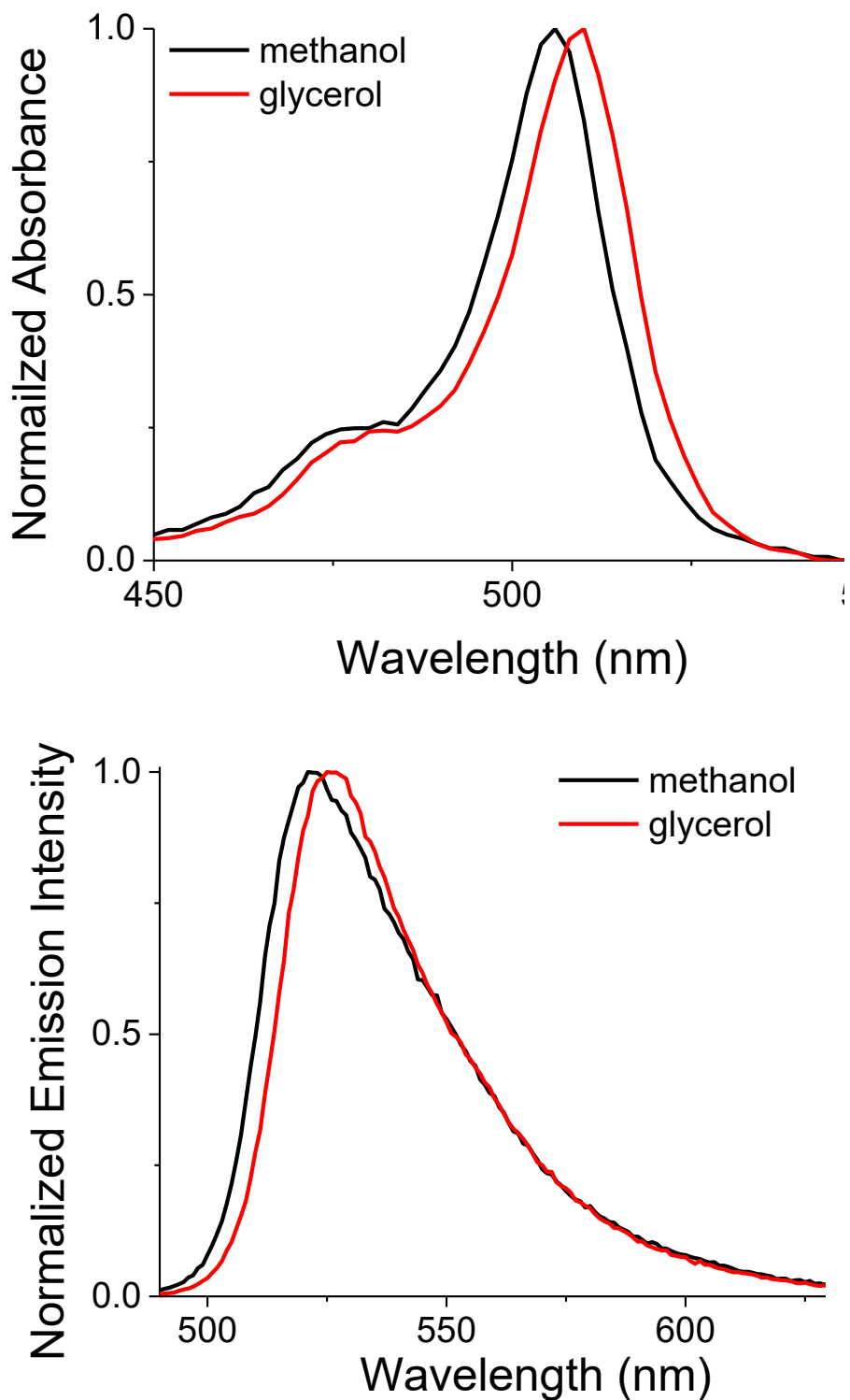


Figure S7. Normalized UV-vis (top) and fluorescence spectra (bottom) of **1b** (5 μ M) in methanol and glycerol, excited at 480 nm.

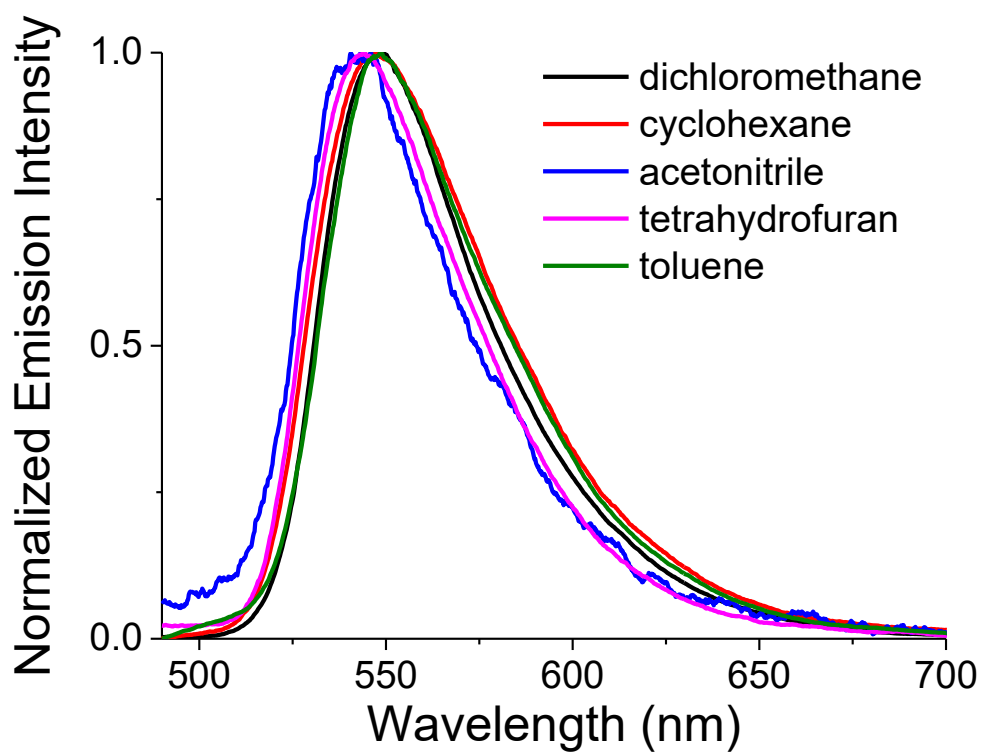
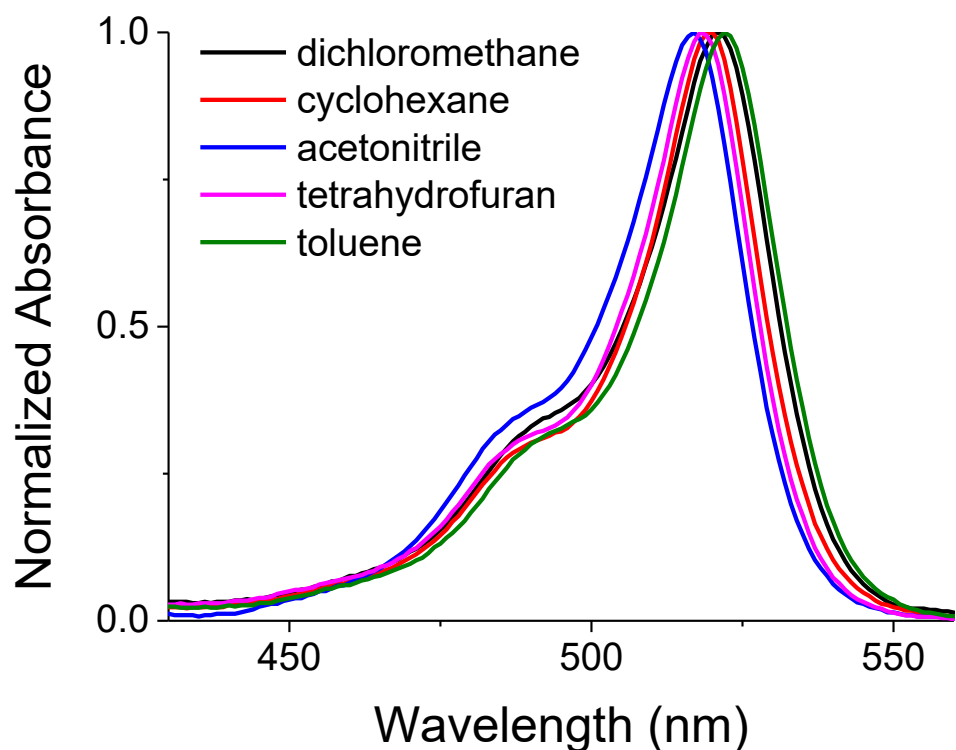


Figure S8. Normalized UV-vis (top) and fluorescence spectra (bottom) of **1c** in different solvents, excited at 480 nm.

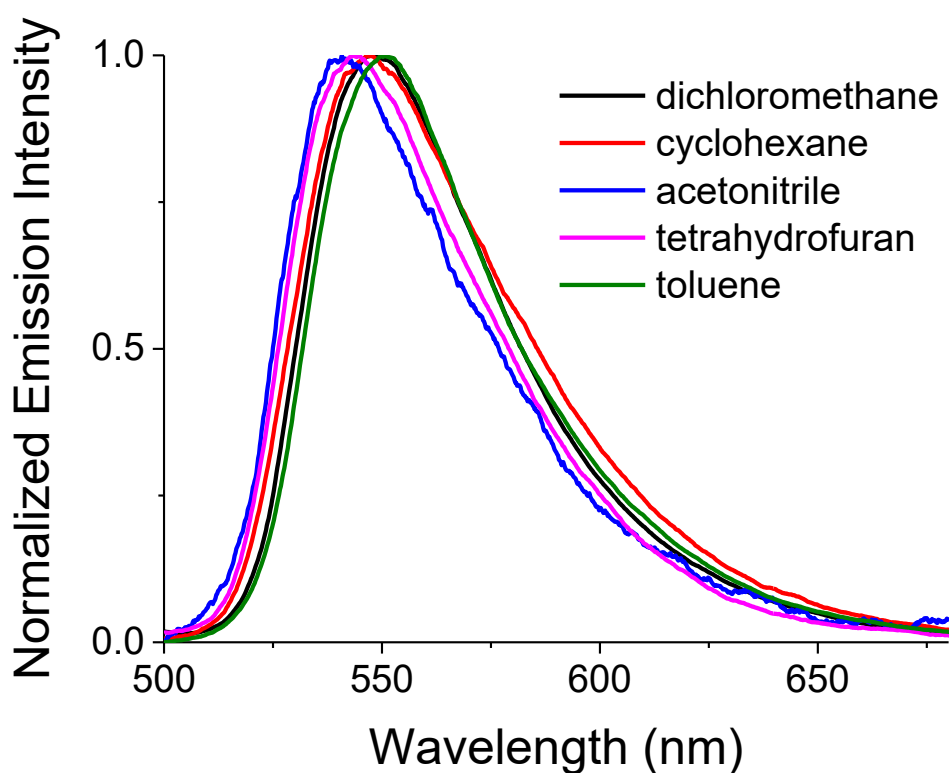
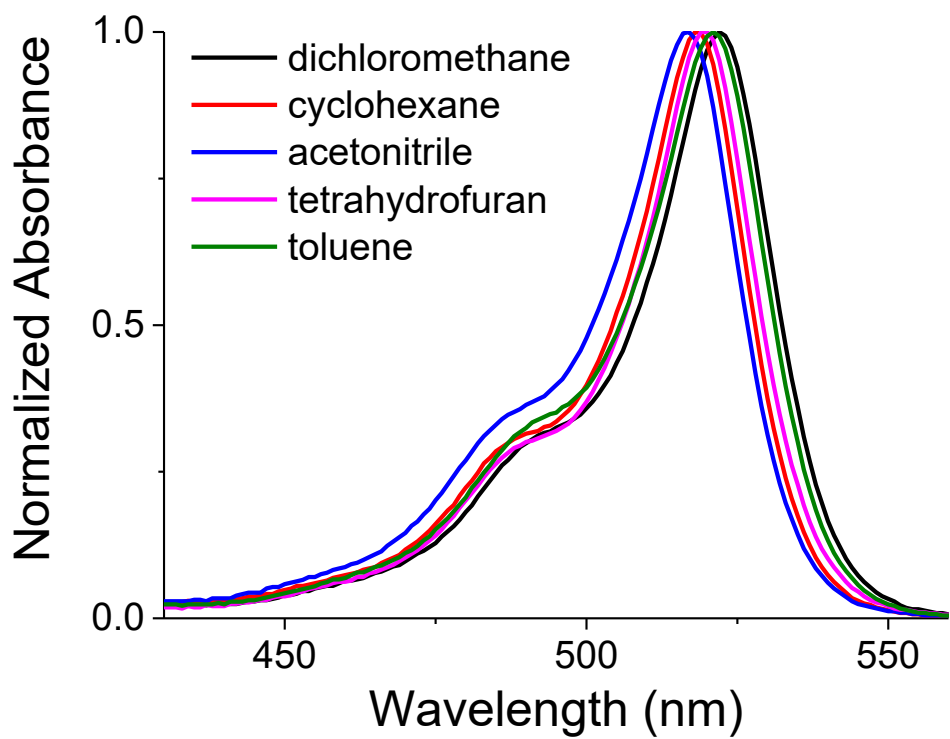


Figure S9. Normalized UV-vis (top) and fluorescence spectra (bottom) of **1d** in different solvents, excited at 480 nm.

3. Aggregation-induced emission properties

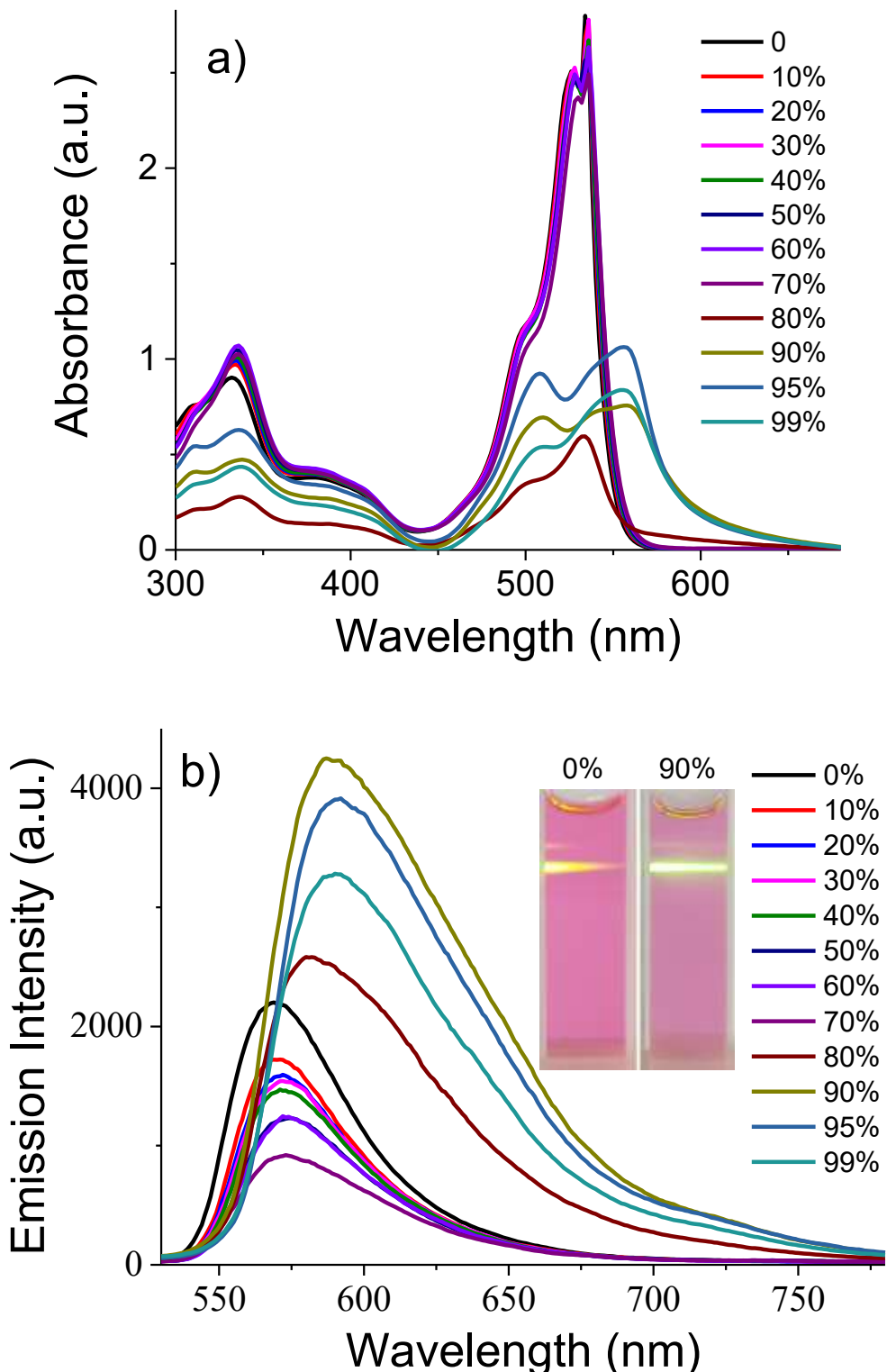


Figure S10. Absorbance (a) and fluorescence (b) spectra of **1a** (50 μ M) in acetonitrile/water with different water fractions (f_w), excited at 500 nm. Photographs of acetonitrile and the mixed acetonitrile-water system containing 90% water of **1a** under 365 nm handheld UV lamp irradiation condition.

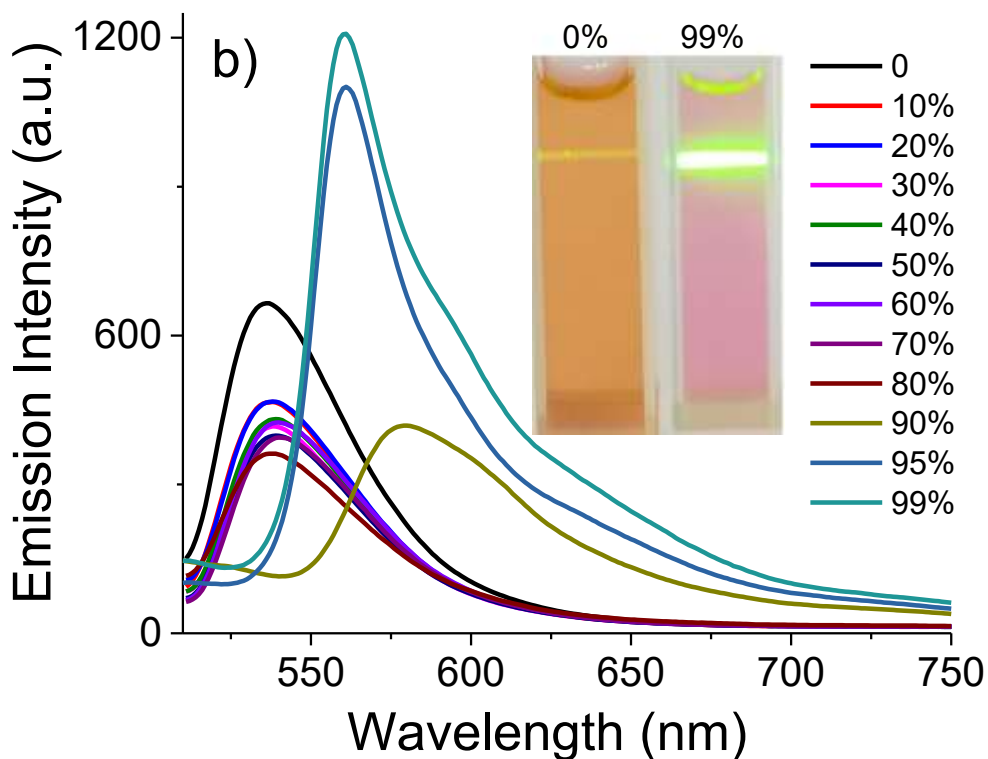
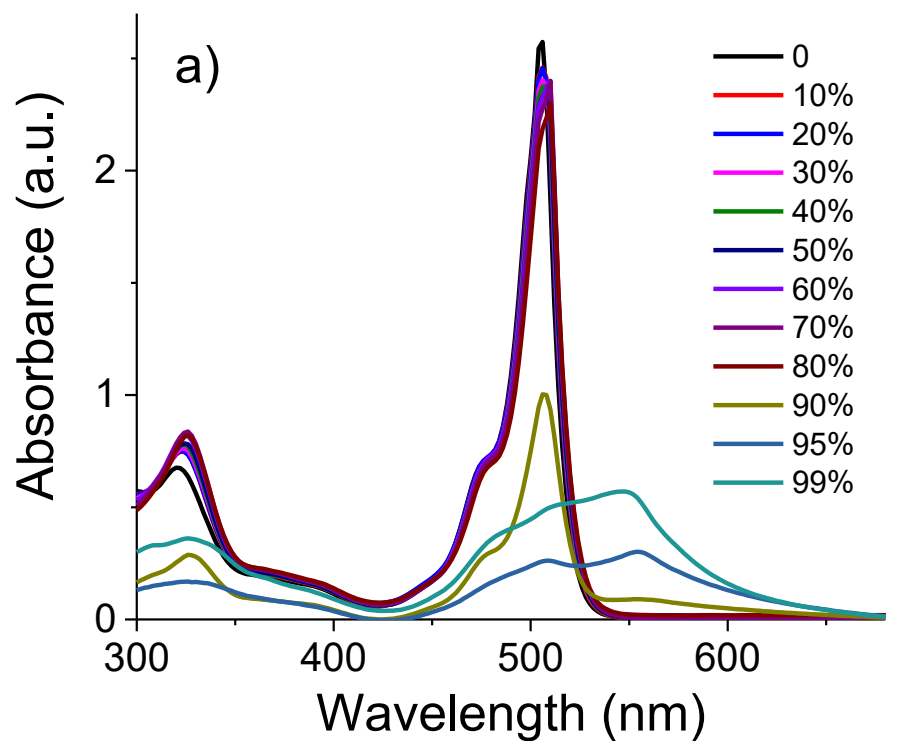


Figure S11. Absorbance (a) and fluorescence (b) spectra of **1b** (30 μ M) in acetonitrile/water with different water fractions (f_w), excited at 480 nm. Photographs of acetonitrile and the mixed acetonitrile-water system containing 99% water of **1b** under 365 nm handheld UV lamp irradiation condition.

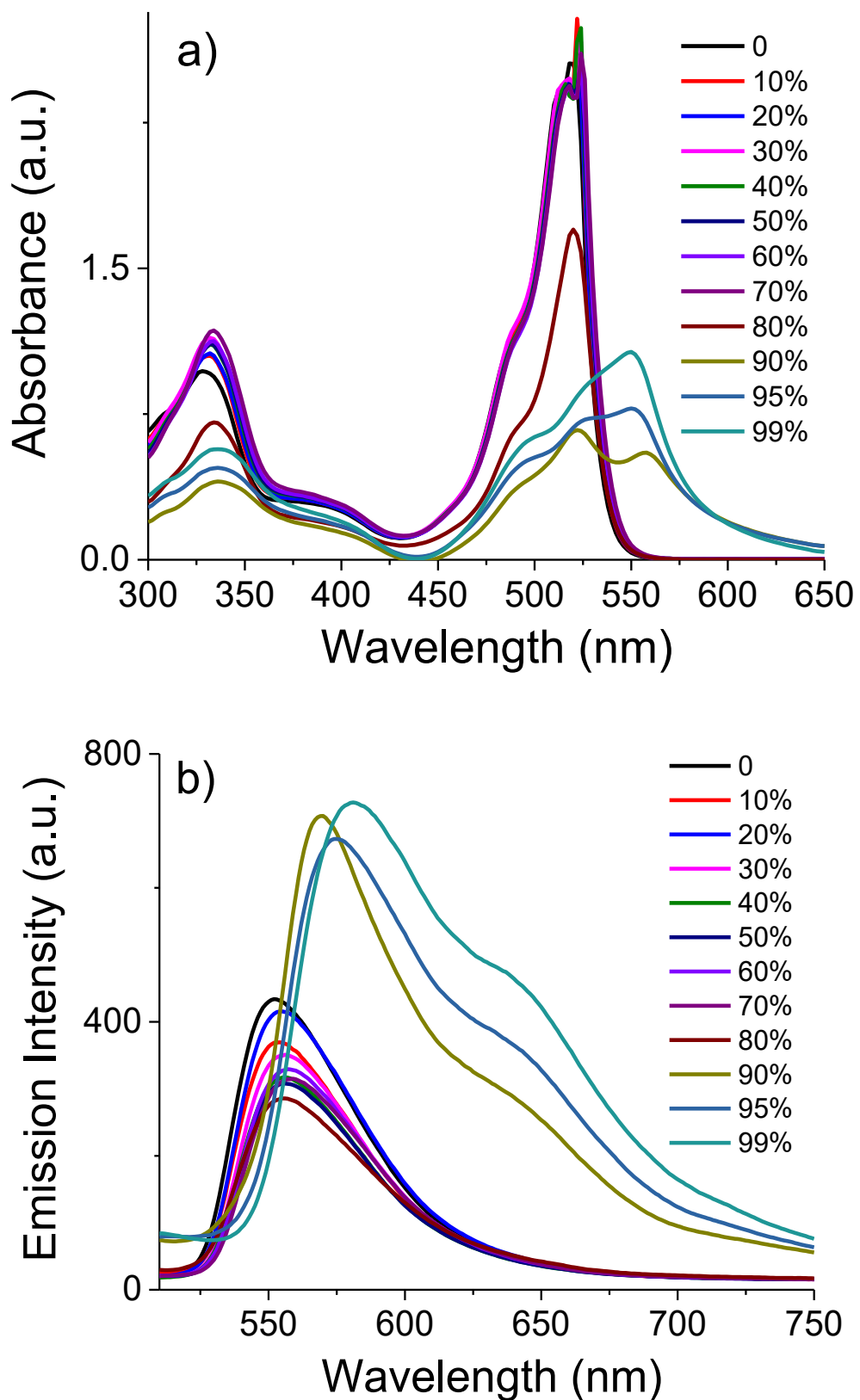


Figure S12. Absorbance (a) and fluorescence (b) spectra of **1c** (30 μ M) in acetonitrile/water with different water fractions (f_w), excited at 480 nm.

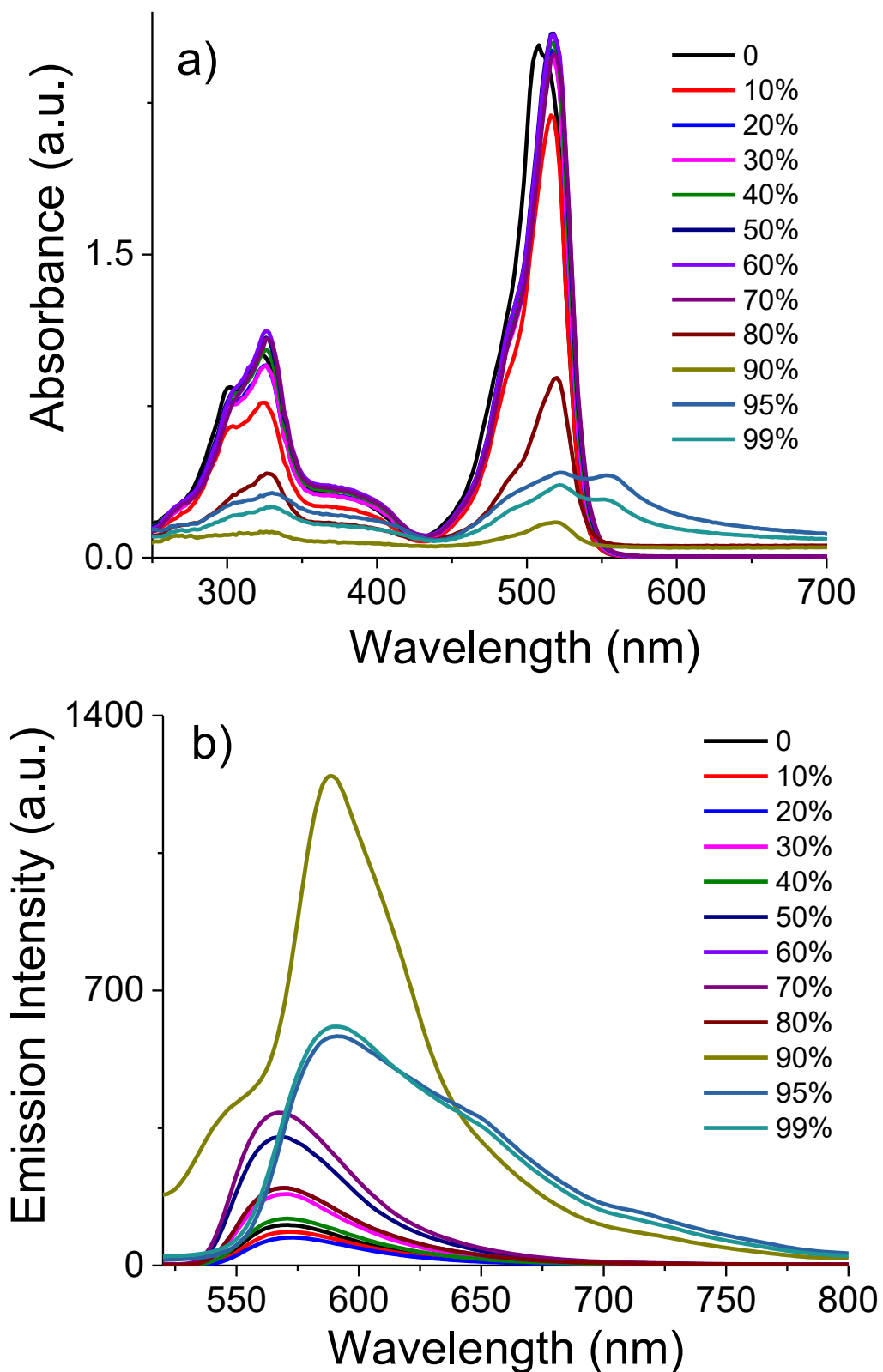


Figure S13. Absorbance (a) and fluorescence (b) spectra of **1d** (30 μM) in acetonitrile/water with different water fractions (f_w), excited at 480 nm.

4. SEM and TEM images

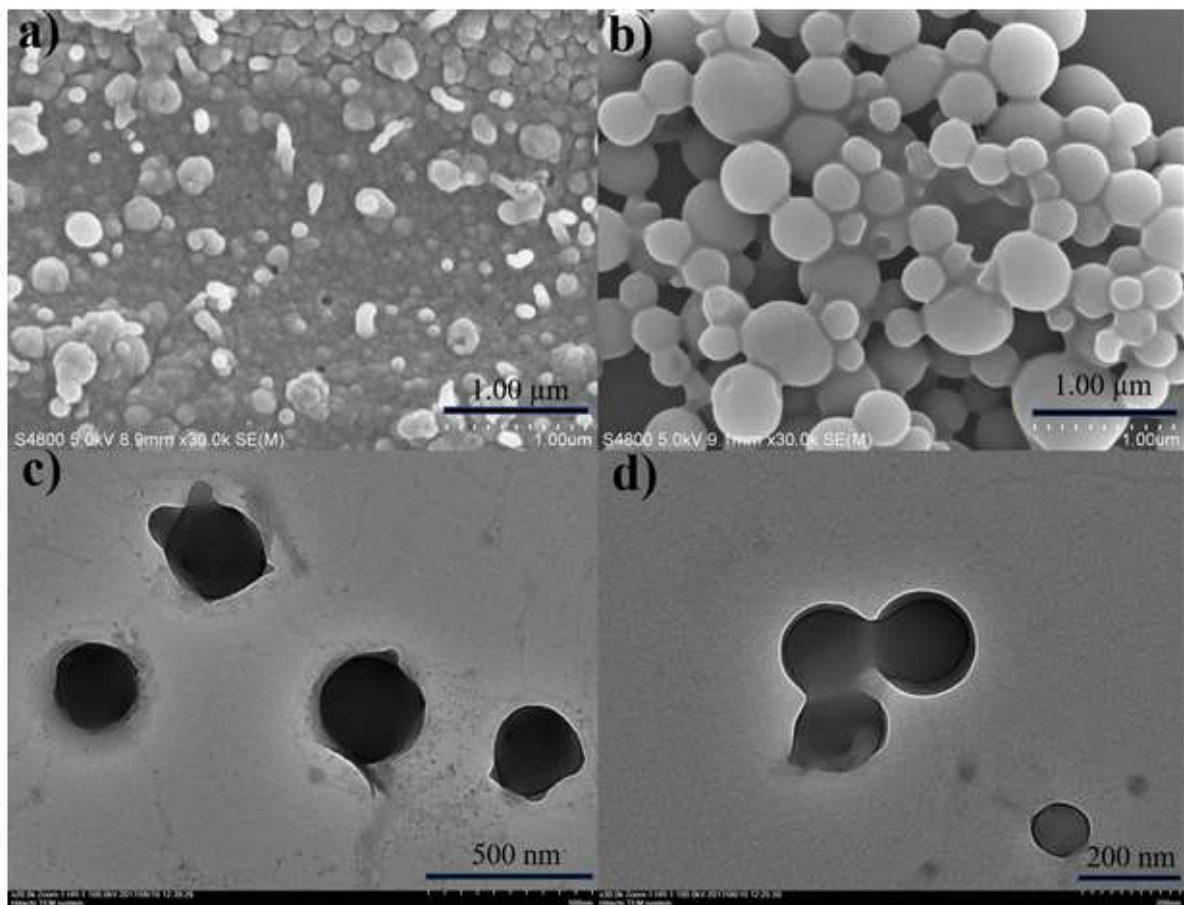


Figure S14. SEM (a, b) and TEM (c, d) images of nanoballs for **1c** (30 μM) and nanocuboid for **1d** (30 μM) in acetonitrile-water system with $f_w = 90\%$.

5. Dynamic light scattering

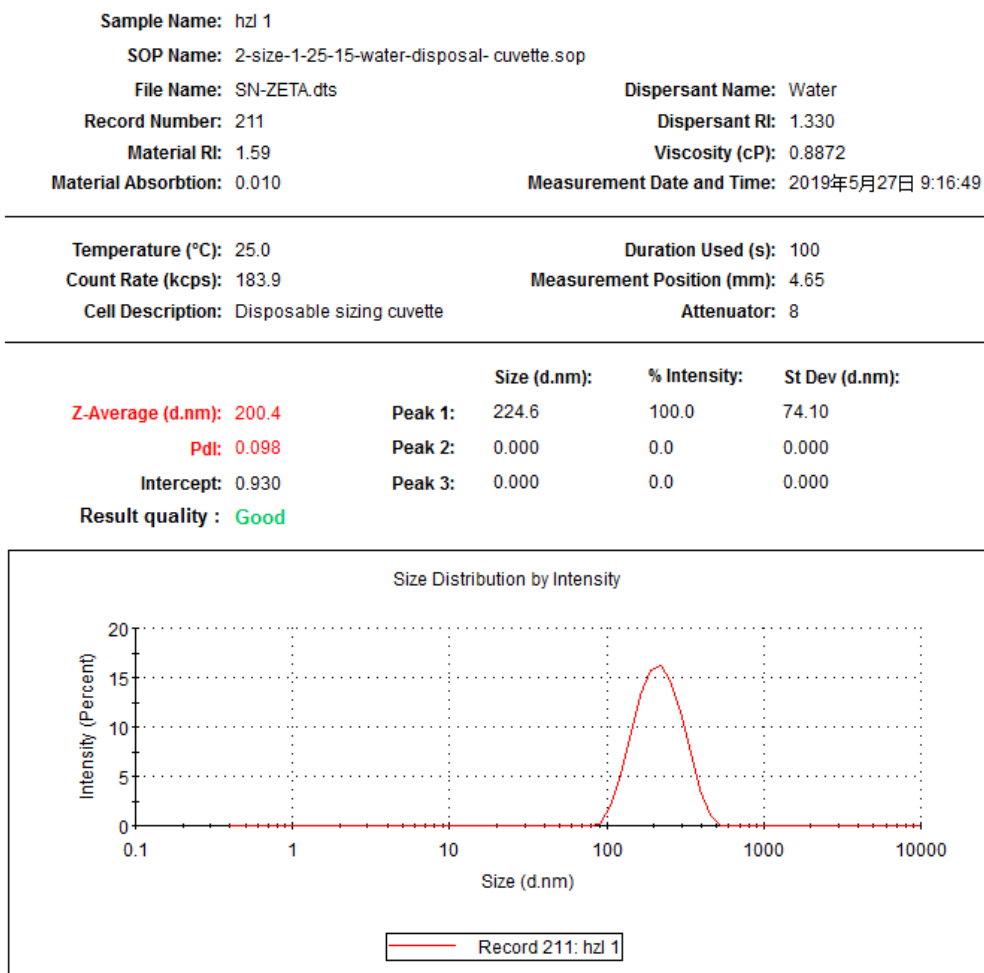


Figure S15. Dynamic light scattering (DLS) of the nanoparticles **1a** (50 μM) in acetonitrile-water system with water fraction equal to 99%.

Sample Name: 11
 SOP Name: 2-size-1-25-15-water-disposal-cuvette.sop
 File Name: dspe-1-zeta.dts
 Record Number: 220
 Material RI: 1.59
 Material Absorbtion: 0.010
 Dispersant Name: Water
 Dispersant RI: 1.330
 Viscosity (cP): 0.8872
 Measurement Date and Time: 2019年5月23日 10:16:19

Temperature (°C): 25.0	Duration Used (s): 100		
Count Rate (kcps): 355.3	Measurement Position (mm): 4.65		
Cell Description: Disposable sizing cuvette			
	Attenuator: 9		
Z-Average (d.nm): 347.1	Size (d.nm):	% Intensity:	St Dev (d.nm):
Pdl: 0.283	Peak 1: 301.3	100.0	68.36
Intercept: 0.825	Peak 2: 0.000	0.0	0.000
Result quality : Good	Peak 3: 0.000	0.0	0.000

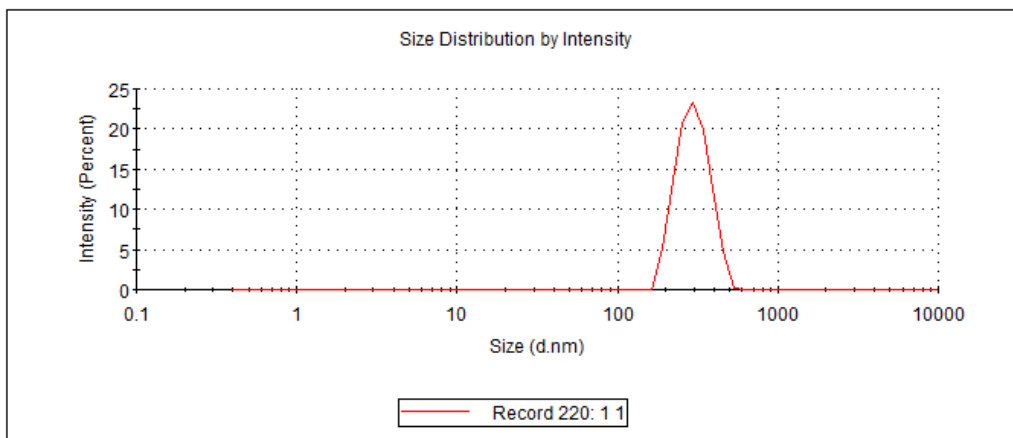


Figure S16. Dynamic light scattering (DLS) of the nanoparticles **1b** (30 μ M) in acetonitrile-water system with water fraction equal to 99%.

6. Viscosity sensitivity studies

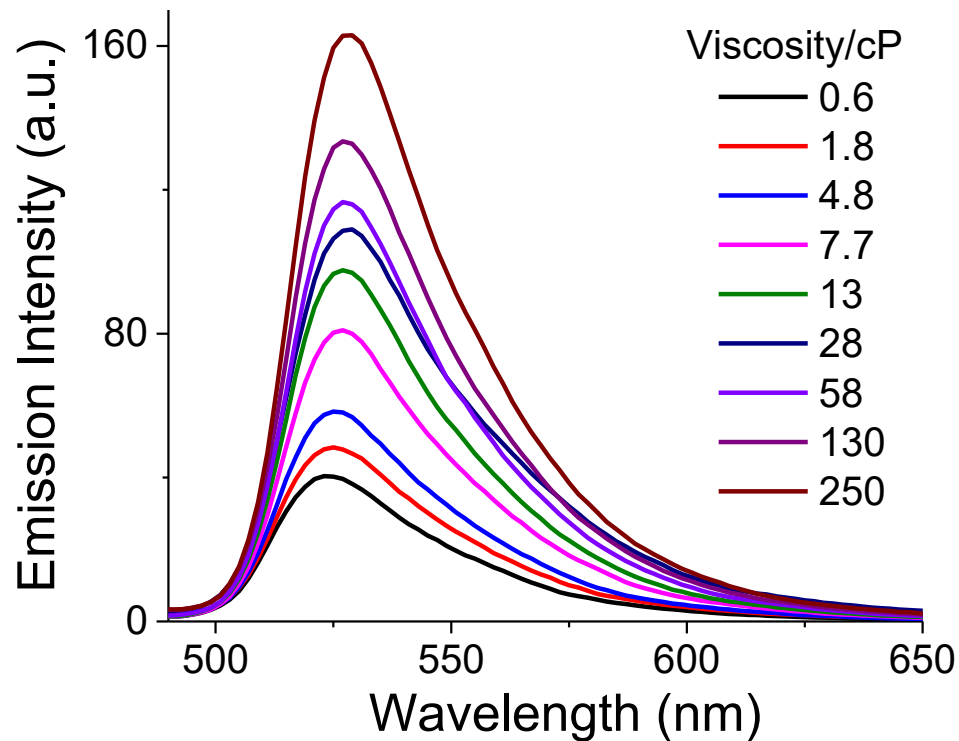


Figure S17. Changes of fluorescence intensity of **1b** (5 μ M, excited at 480 nm) in methanol-glycerol system with the variation of solution viscosity.

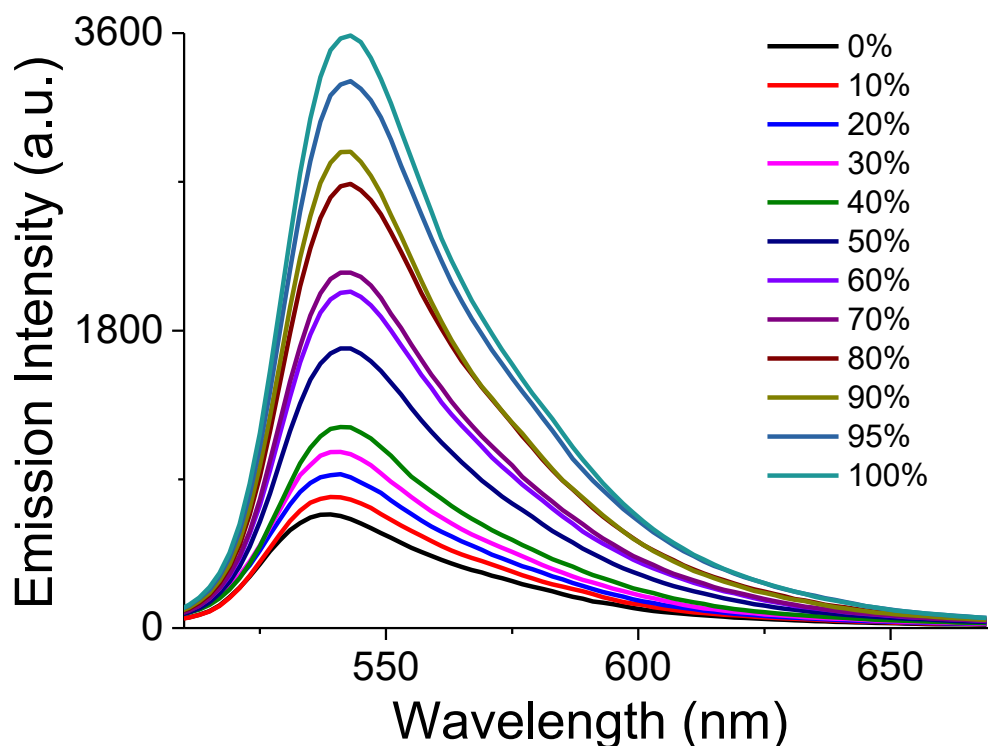


Figure S18. Viscosity change of the absorbance and fluorescence emission spectra of **1c** (5 μ M) in methanol-glycerol mixtures, excited at 500 nm.

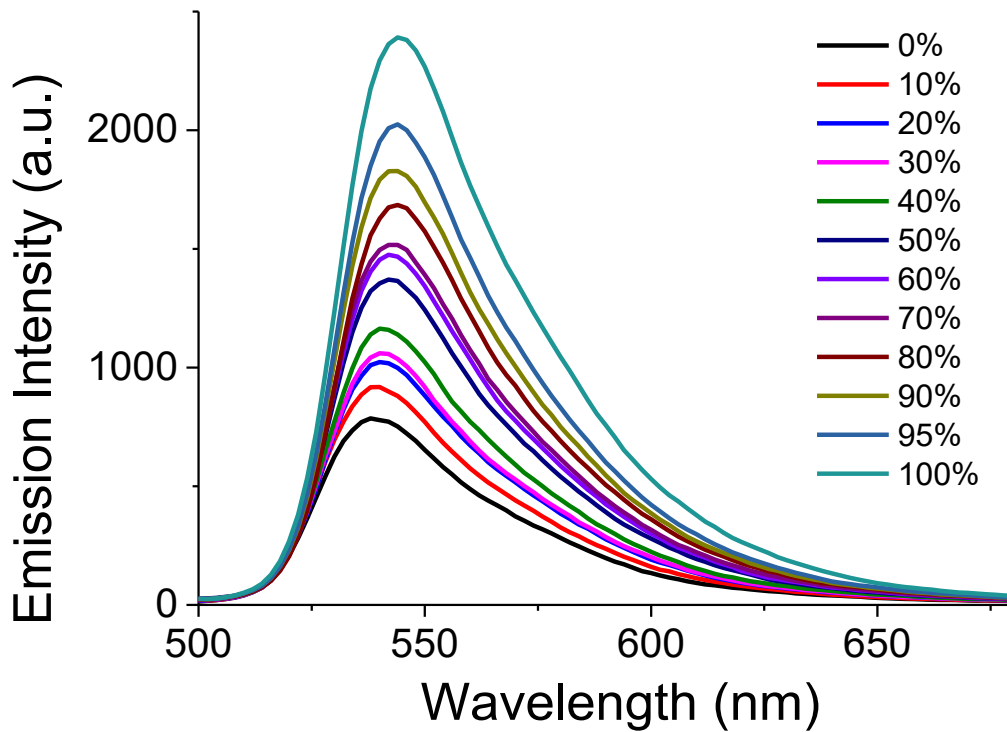


Figure S19. Viscosity change of the absorbance and fluorescence emission spectra of **1d** (5 μM) in methanol-glycerol mixtures, excited at 480 nm.

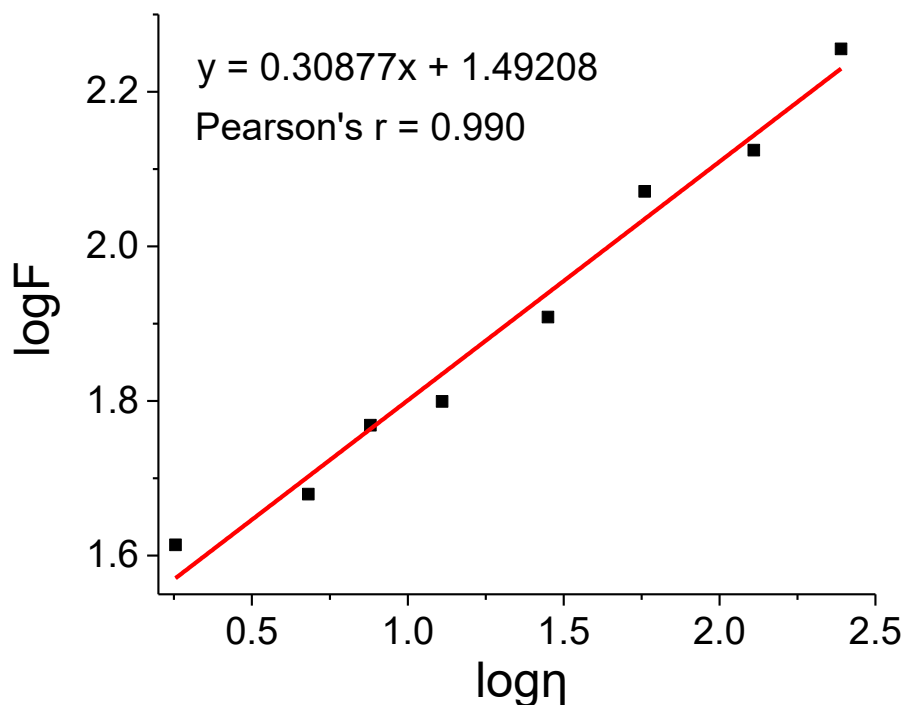


Figure S20. The linear relationship of **1b** between the fluorescent intensity and the viscosity η .

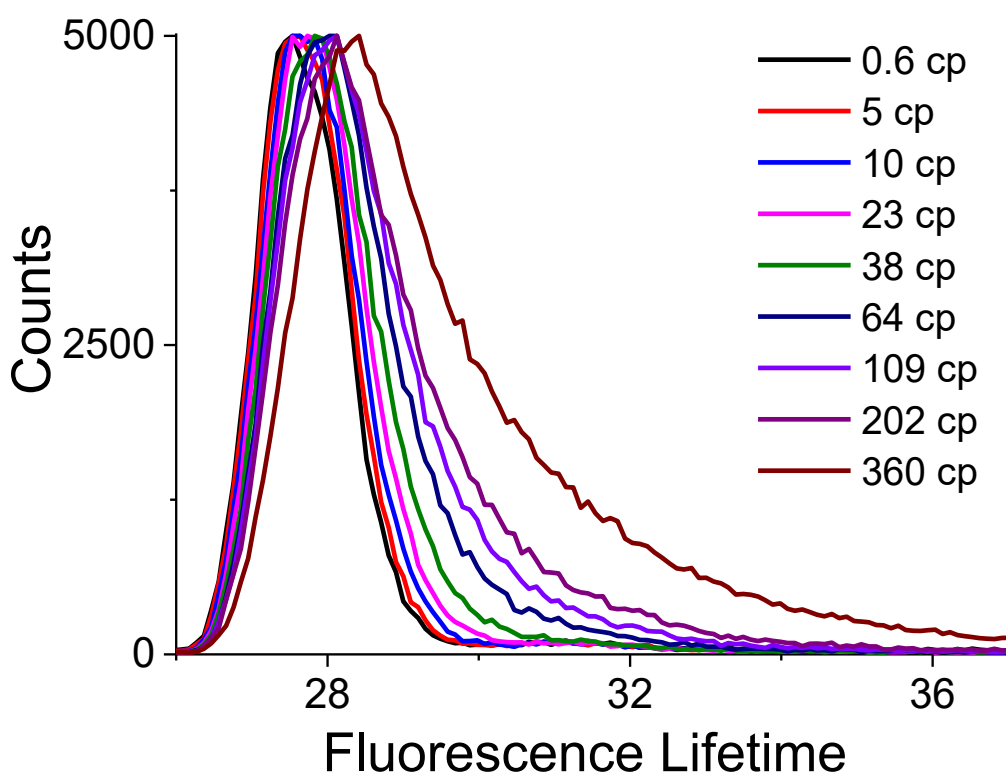


Figure S21. The fluorescence lifetime spectra of **1b** with different viscosity collected at 560 nm.

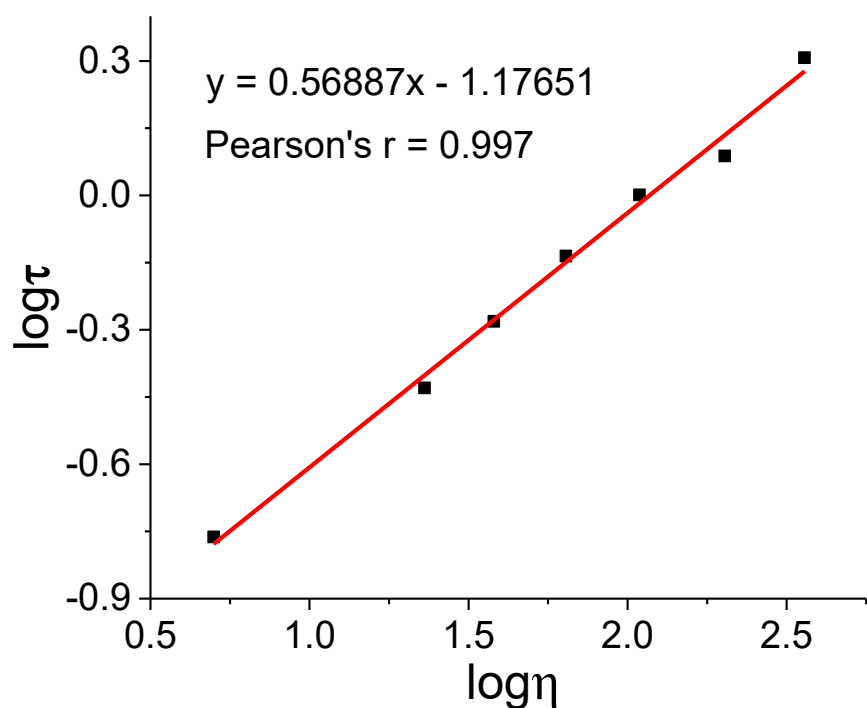


Figure S22. The linear relationship of **1b** between the fluorescence lifetime and the viscosity η .

7. Cell culture

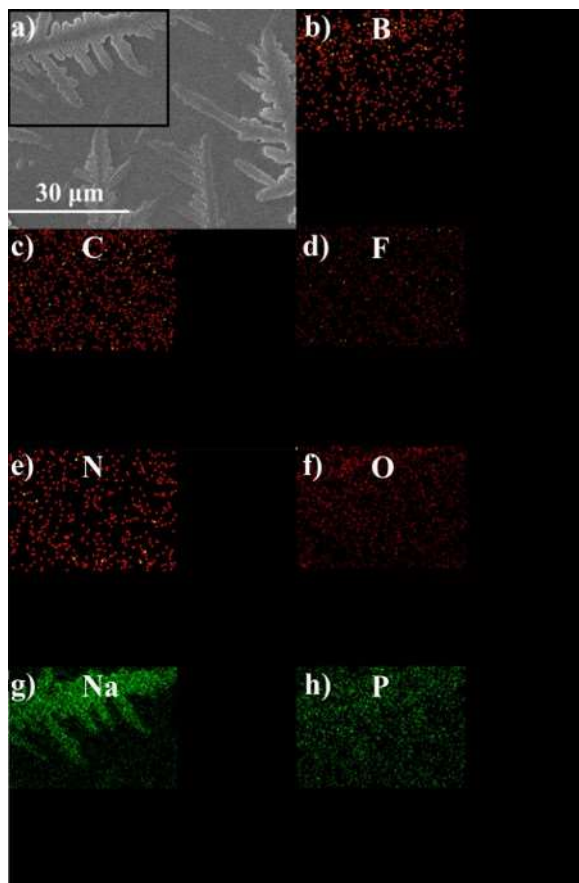


Figure S23. a) SEM image of BODIPY **1a** (5 μM) in phosphate-buffered saline (PBS) and EDS mapping in the rectangle frame for B (b), C (c), F (d), N (e), O (f), Na (g) and P (h).

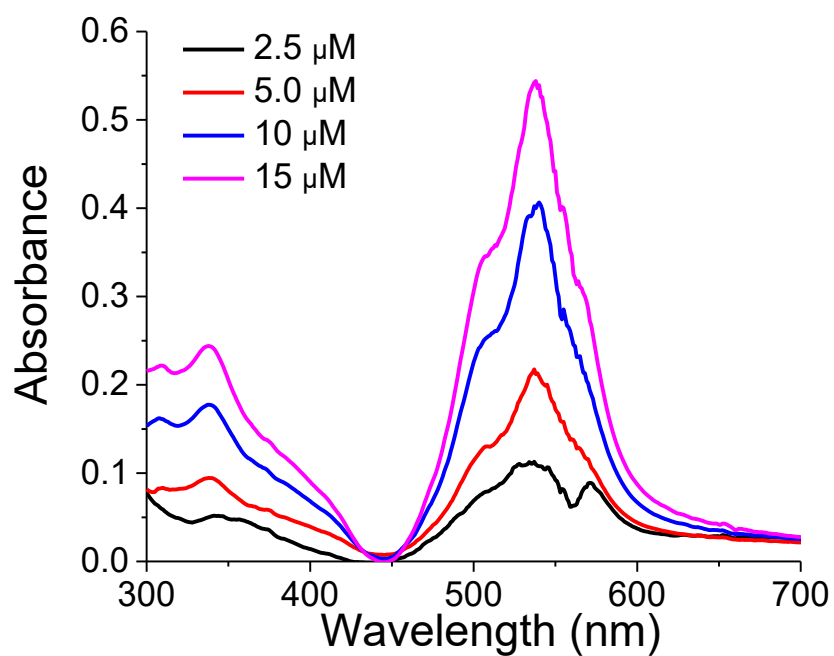


Figure S24. Absorbance of BODIPY **1a** with different concentrations of 2.5 μM , 5 μM , 10 μM and 15 μM in dulbecco's modified eagle medium (DMEM).

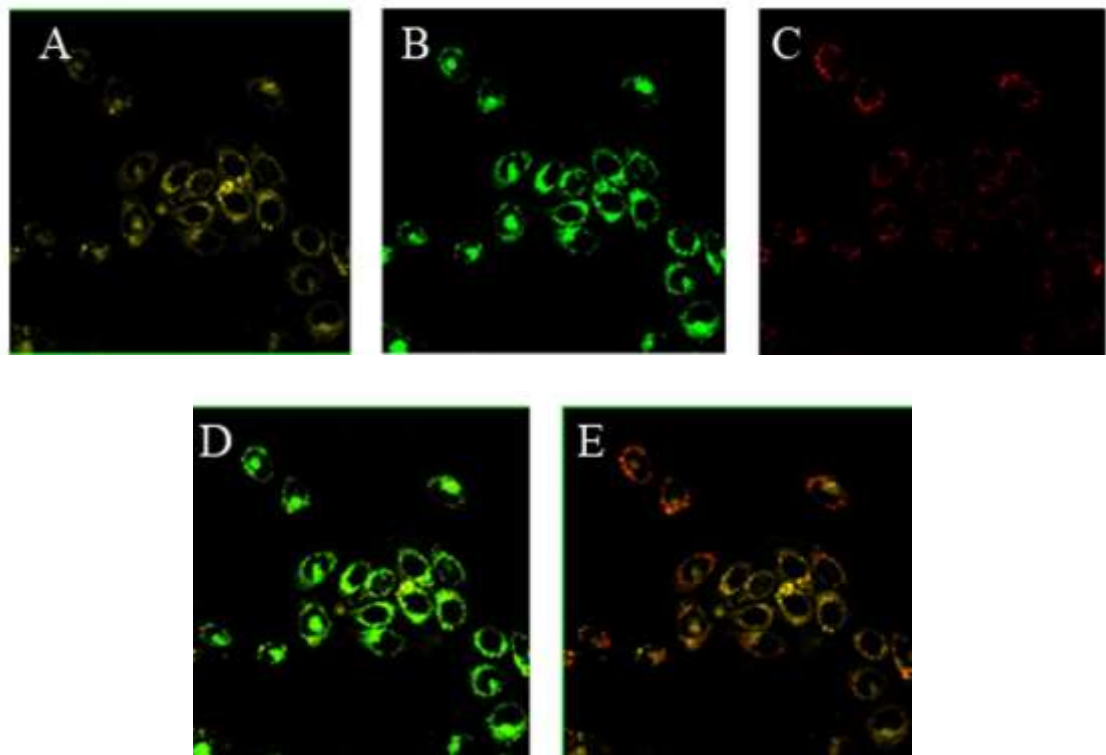


Figure 25. Co-location imaging studies in MCF-7 cells: (A) Stained with **1a** ($5 \mu\text{M}$, $\lambda_{\text{ex}} = 515 \text{ nm}$, $\lambda_{\text{em}} = 520\text{-}600 \text{ nm}$); (B) Stained with DND-99 ($1 \mu\text{M}$, $\lambda_{\text{ex}} = 559 \text{ nm}$, $\lambda_{\text{em}} = 575\text{-}620 \text{ nm}$); (C) Stained with Mito Deep Red ($1 \mu\text{M}$ $\lambda_{\text{ex}} = 635 \text{ nm}$, $\lambda_{\text{em}} = 655\text{-}755 \text{ nm}$); (D) Merge of A and B; (E) Merge of A and C.

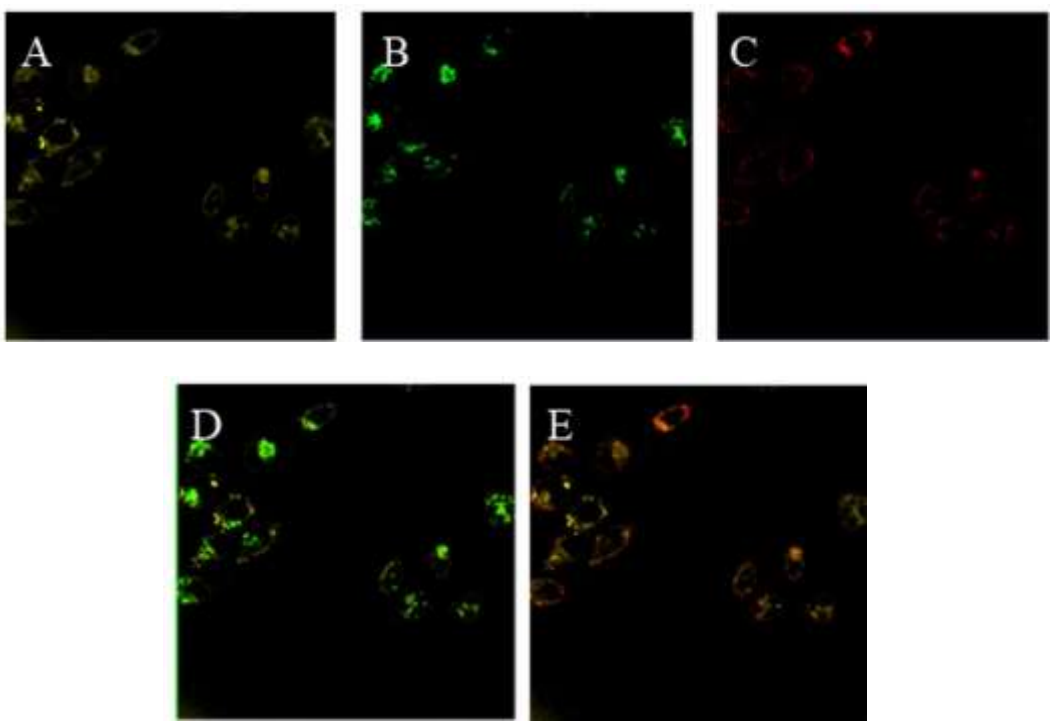


Figure 26. Co-location imaging studies in MCF-7 cells: (A) Stained with **1b** ($5 \mu\text{M}$, $\lambda_{\text{ex}} = 515 \text{ nm}$, $\lambda_{\text{em}} = 520\text{-}600 \text{ nm}$); (B) Stained with DND-99 ($1 \mu\text{M}$, $\lambda_{\text{ex}} = 559 \text{ nm}$, $\lambda_{\text{em}} = 575\text{-}620 \text{ nm}$); (C) Stained with Mito Deep Red ($1 \mu\text{M}$, $\lambda_{\text{ex}} = 635 \text{ nm}$, $\lambda_{\text{em}} = 655\text{-}755 \text{ nm}$); (D) Merge of A and B; (E) Merge of A and C.

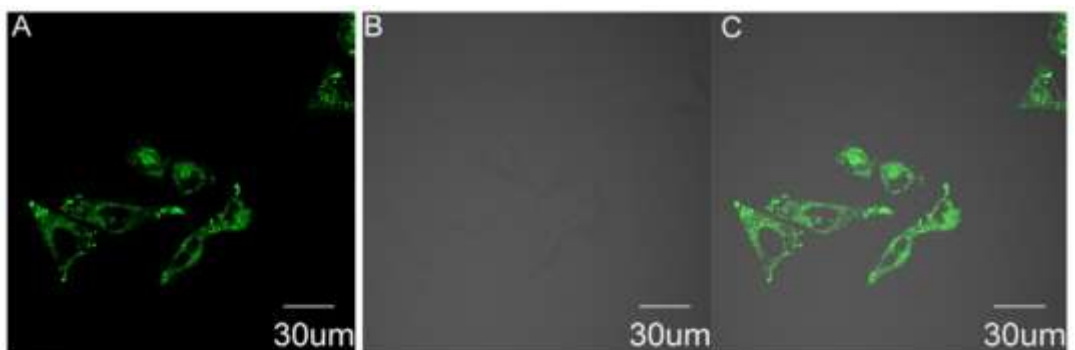


Figure S27. Imaging of **1b** in MCF-7 cells. (A) MCF-7 cells were stained with **1b** ($5 \mu\text{M}$, $\lambda_{\text{ex}} = 488 \text{ nm}$, $\lambda_{\text{em}} = 510\text{-}600 \text{ nm}$); (B) DIC image; (C) Merge of A and B.

8. MTT Assay

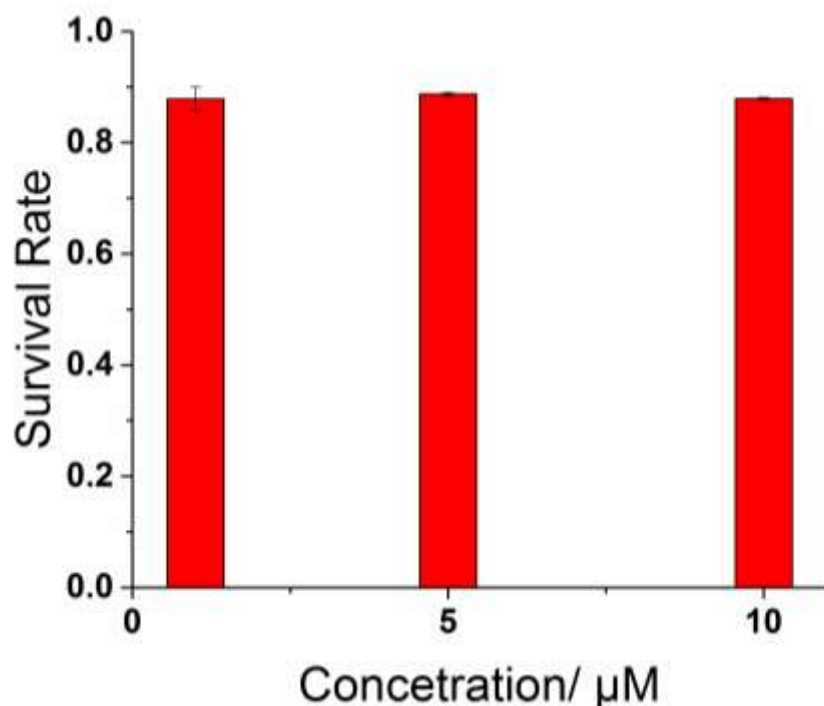


Figure S28. Cell viability of **1a** at different concentrations.

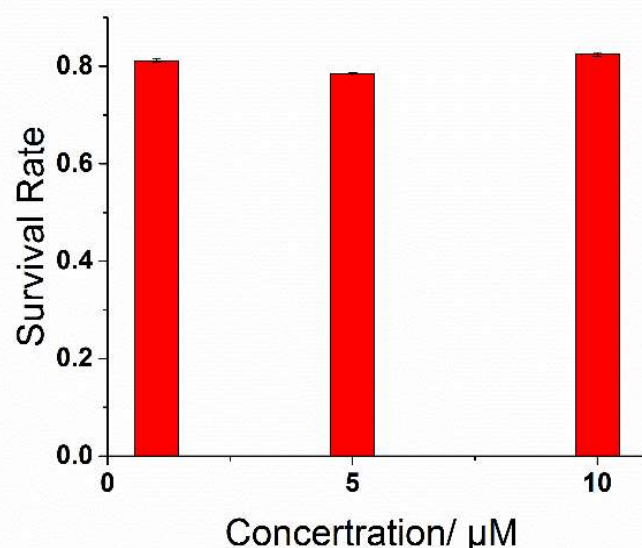


Figure S29. Cell viability of **1b** at different concentrations.

9. Viscosity determination in real-time during apoptosis

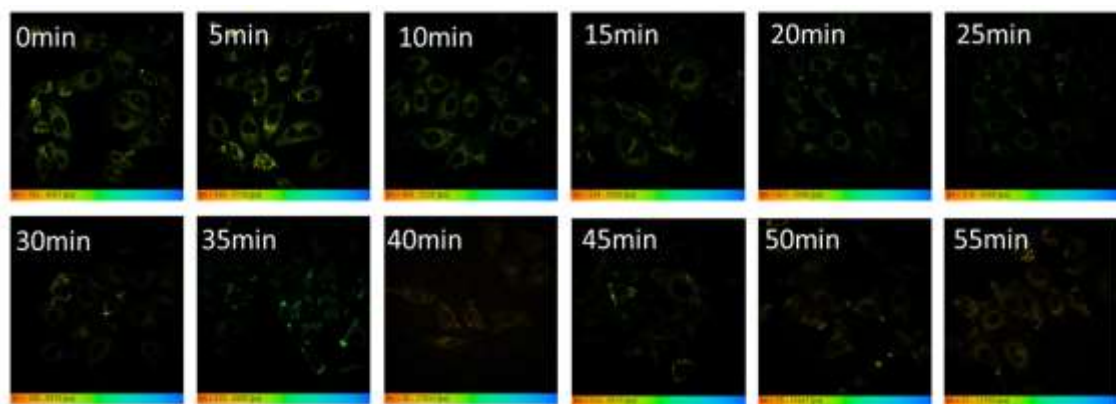


Figure S30. FLIM of MCF-7 cells in the absence and presence of etoposide for 0-60 min (A-E); (G) Plots of fluorescence lifetimes of **1a** (5 μ M) stimulate for different times using etoposide.

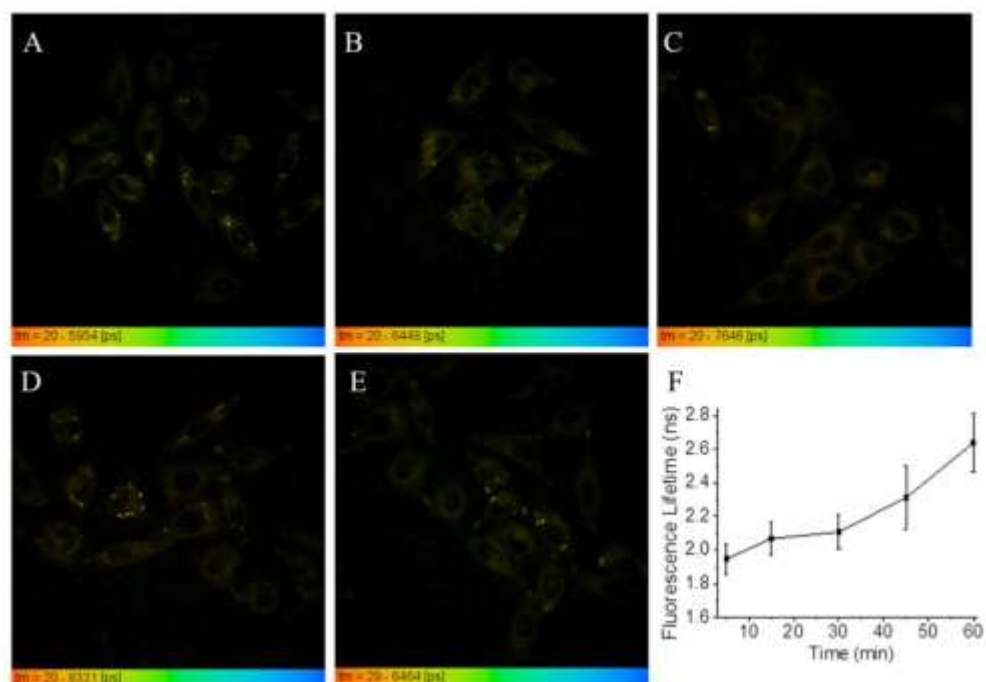
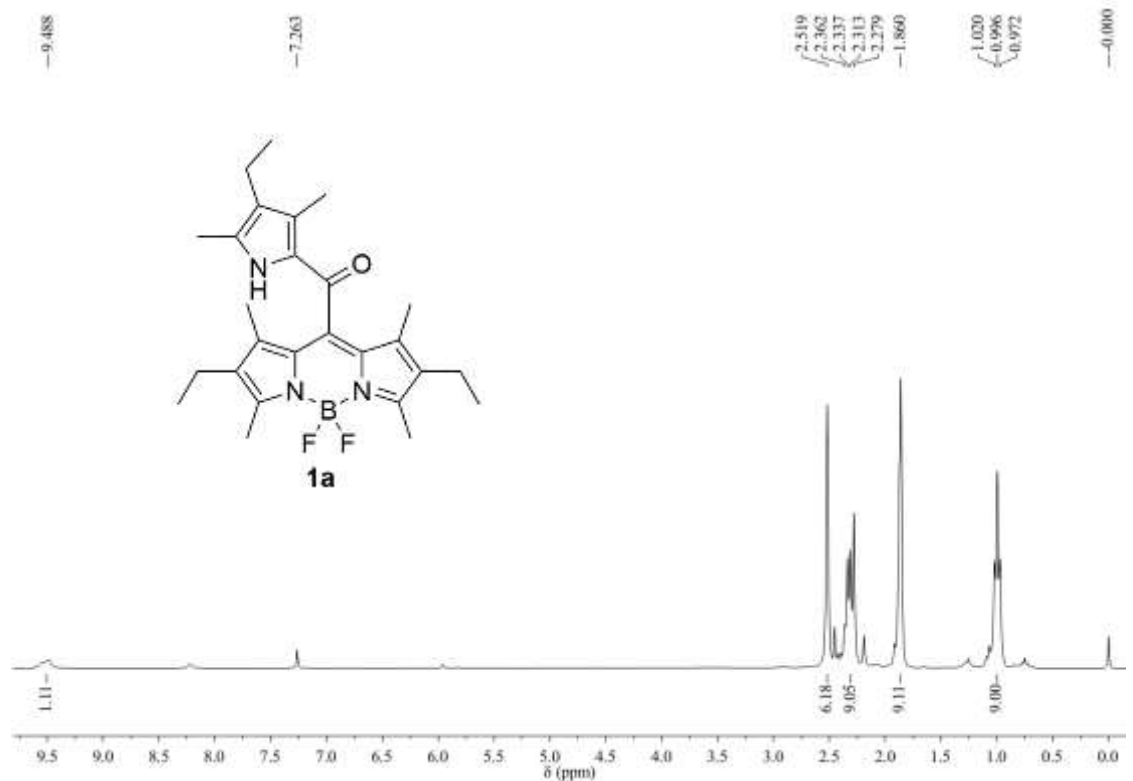
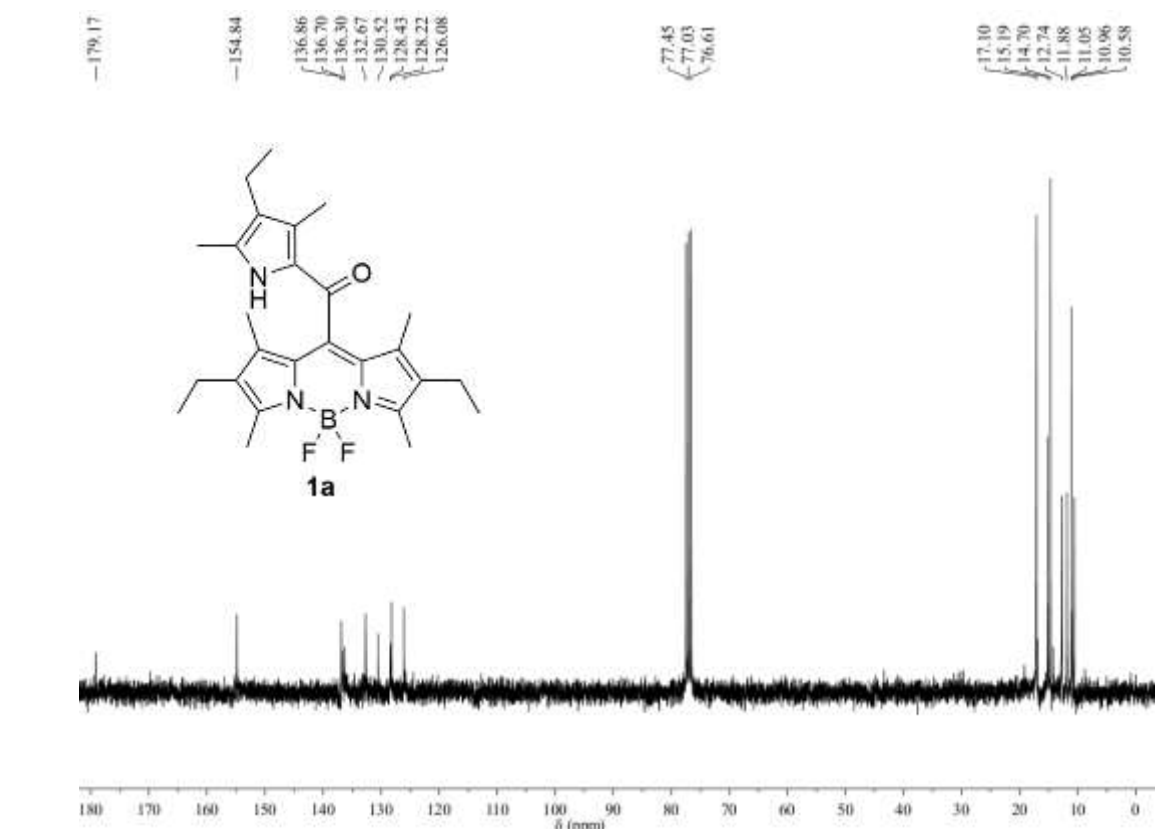


Figure S31. FLIM of MCF-7 cells in the absence and presence of etoposide for 0-60 min (A-E); (G) Plots of fluorescence lifetimes of **1b** (5 μ M) stimulate for different times using etoposide.

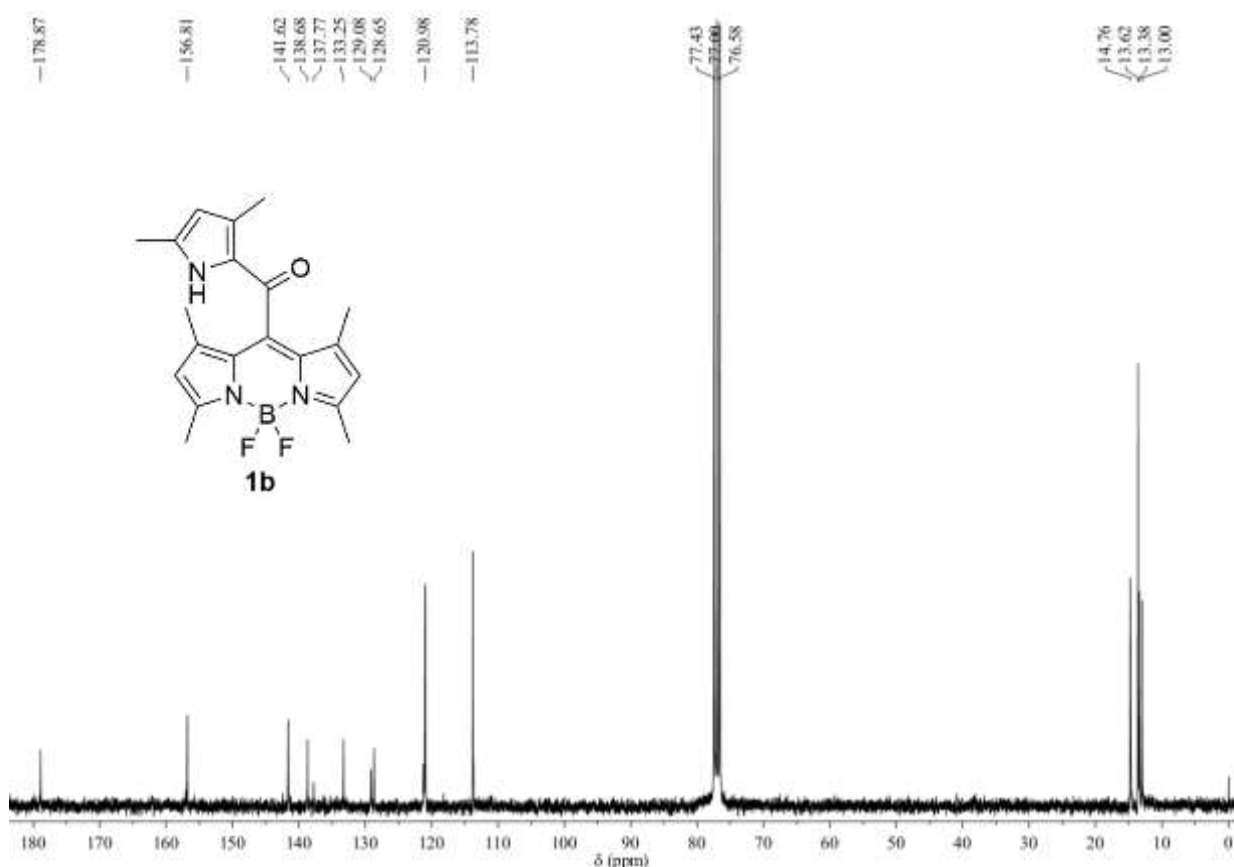
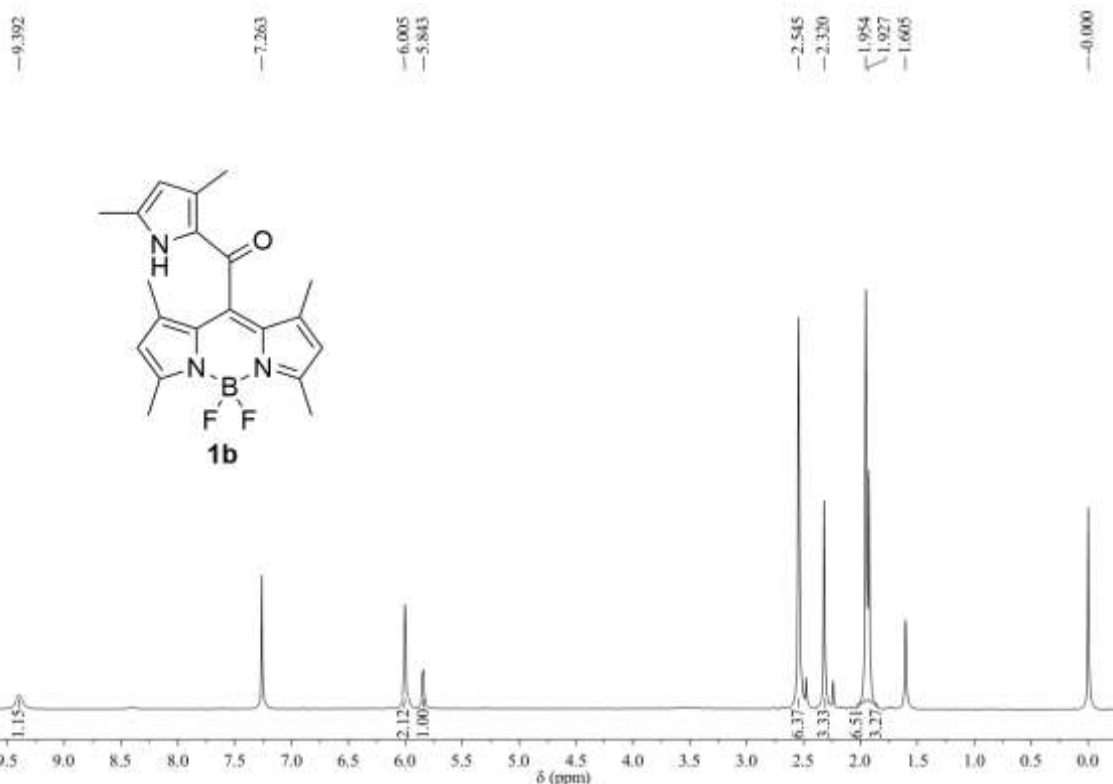
10. NMR spectra for *meso*-2-ketopyrrolyl BODIPYs

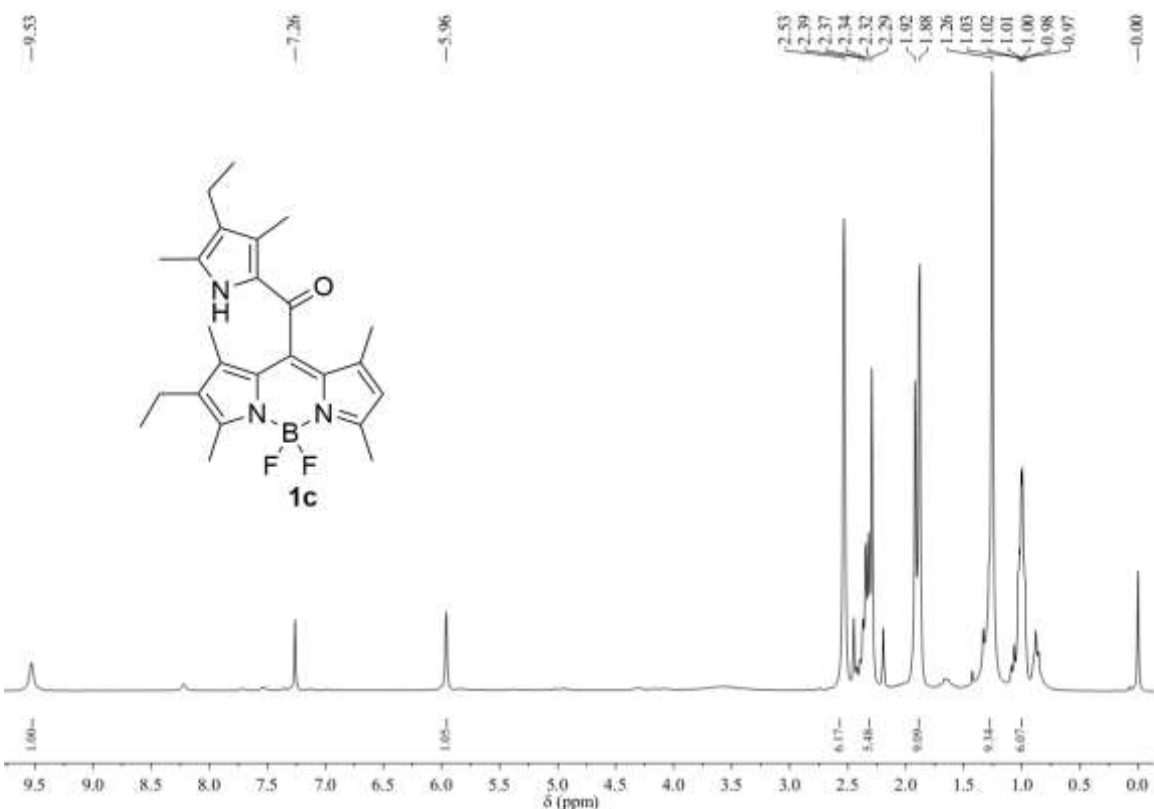


¹H NMR spectrum of meso-2-ketopyrrolyl derived BODIPY **1a** in CDCl₃

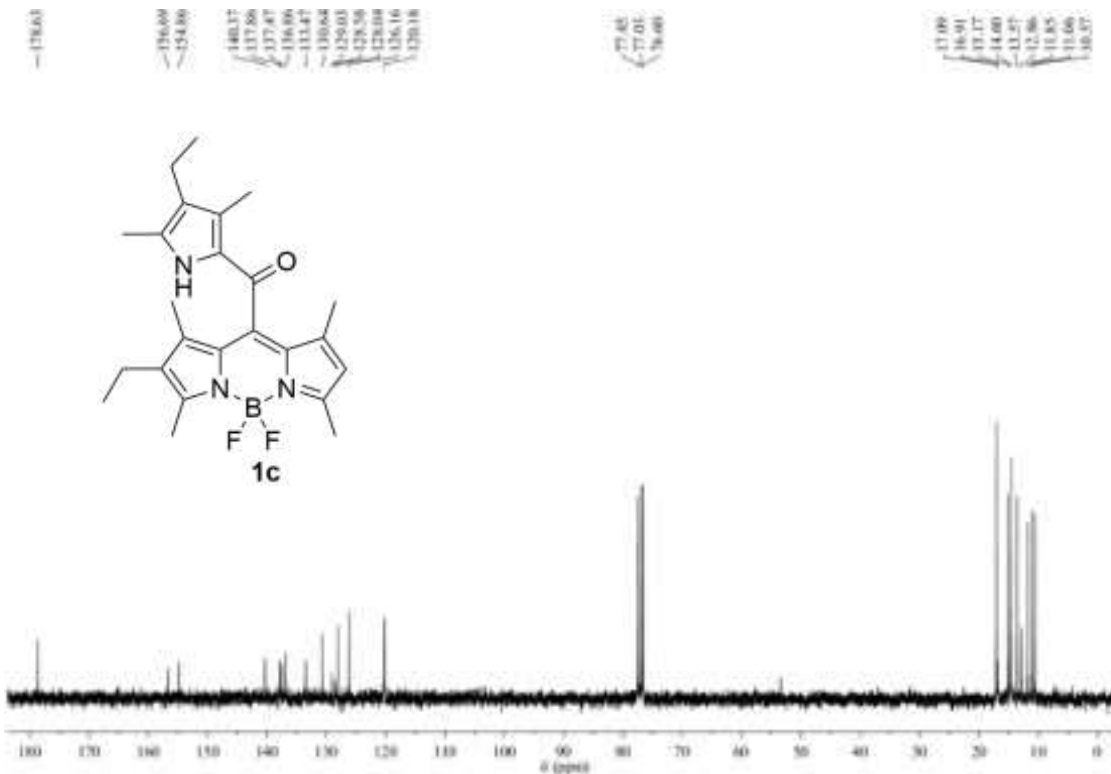


¹³C NMR spectrum of *meso*-2-ketopyrrolyl derived BODIPY **1a** in CDCl₃

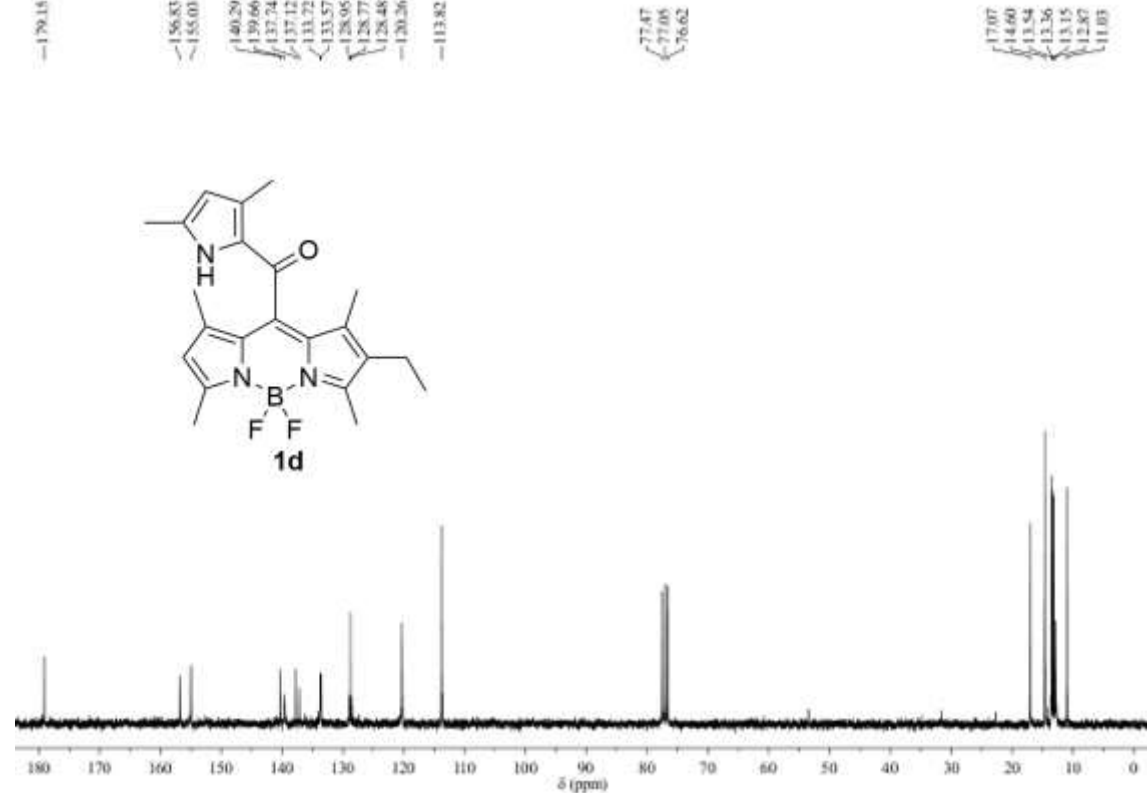
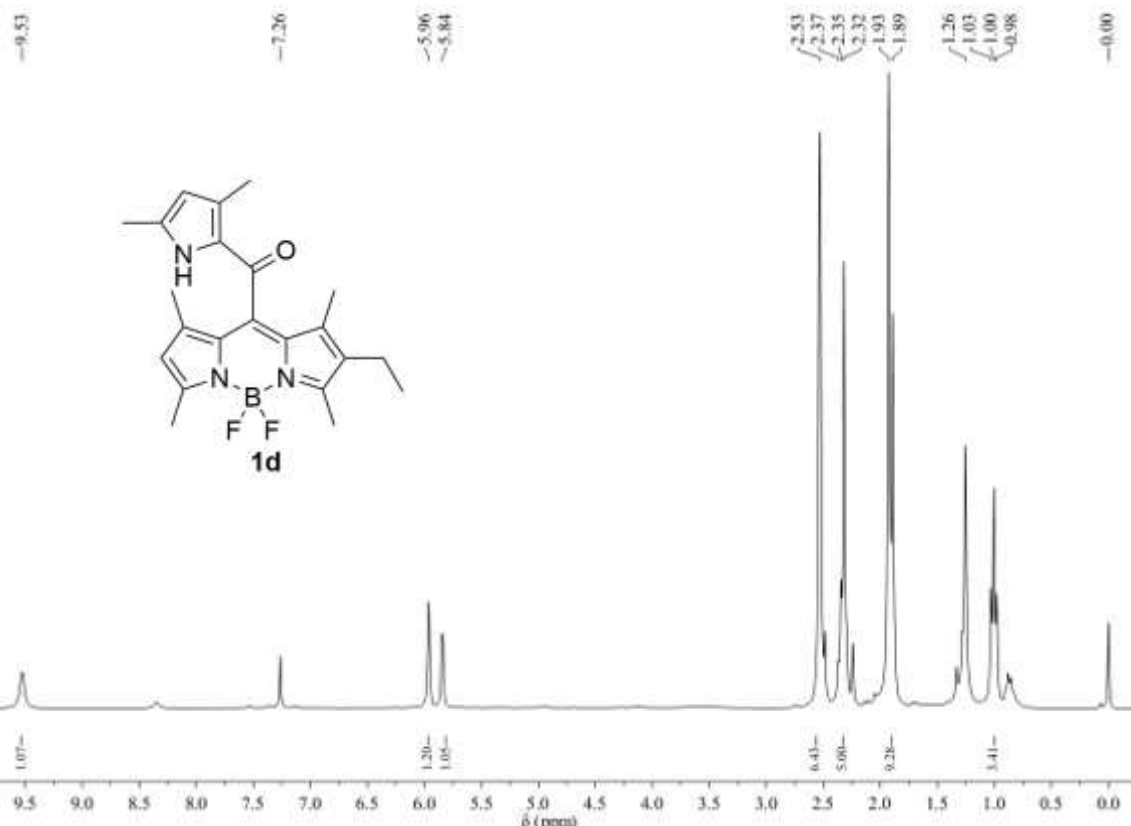




¹H NMR spectrum of *meso*-2-ketopyrrolyl derived BODIPY **1c** in CDCl_3 solution



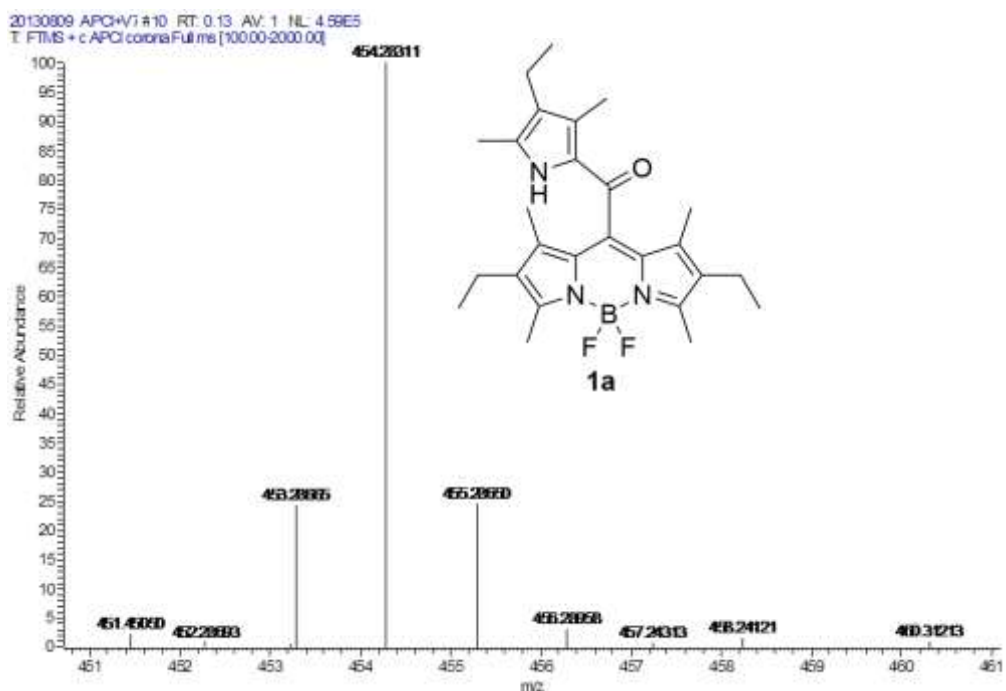
¹³C NMR spectrum of *meso*-2-ketopyrrolyl derived BODIPY **1c** in CDCl_3 solution



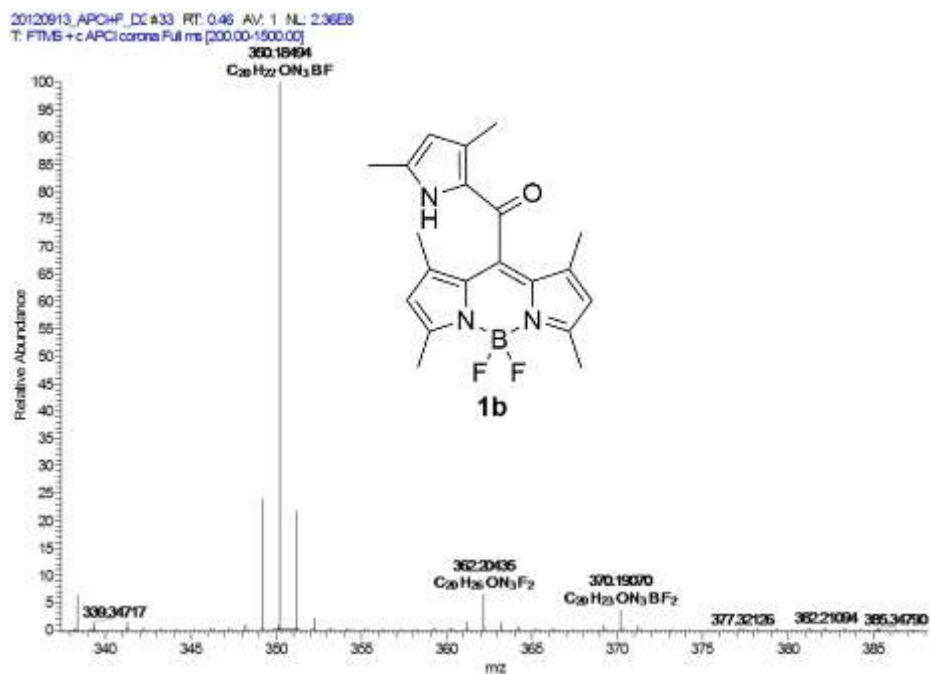
¹³C NMR spectrum of *meso*-2-ketopyrrolyl derived BODIPY **1d** in CDCl_3 solution

11. HRMS for *meso*-2-ketopyrrolyl derived BODIPYs

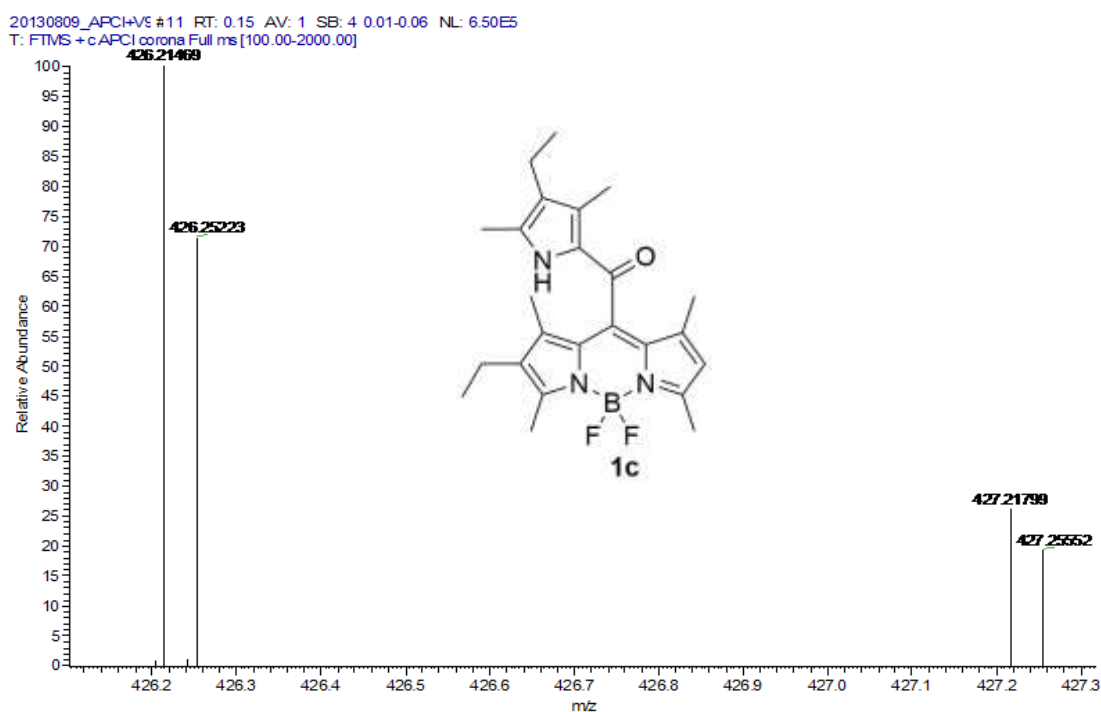
HRMS of 1a



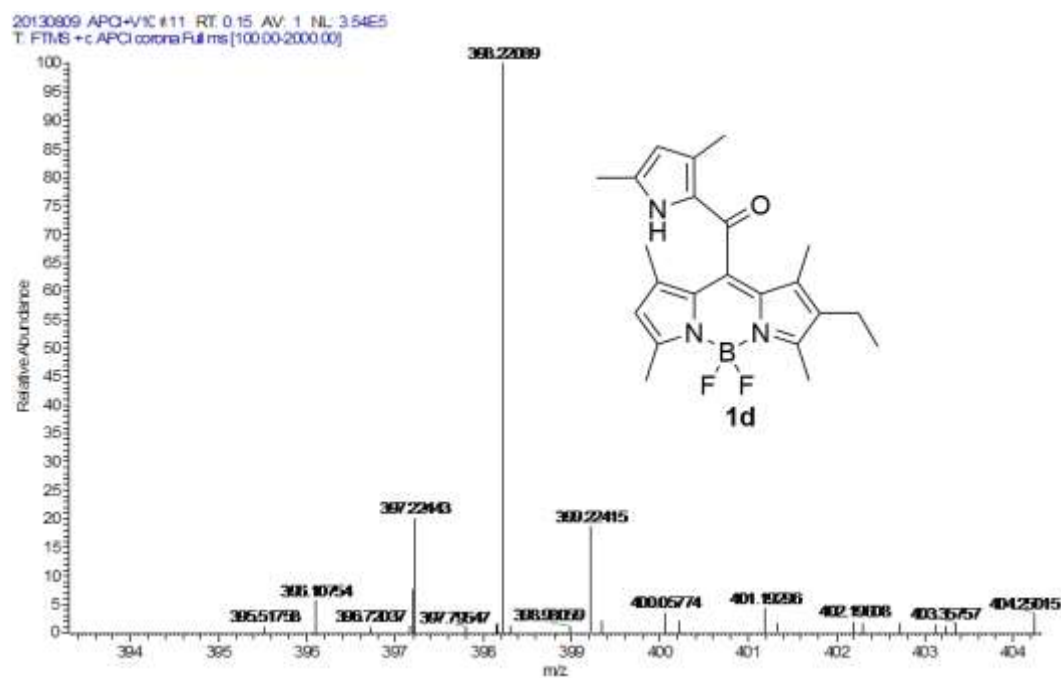
HRMS of 1b



HRMS of *meso*-2-ketopyrrolylBODIPY **1c**



HRMS of *meso*-2-ketopyrrolylBODIPY **1d**



12. DFT computations

Table S4. Selected electronic excitation energies (eV) and oscillator strengths (f), configurations of the low-lying excited states of *meso*-2-ketopyrrolyl BODIPYs **1a** calculated by TDDFT//B3LYP/6-31+G(d,p), based on the optimized ground state geometries. The TDDFT calculations of all the molecules in dichloromethane were done by using the Self-Consistent Reaction Field method and the Polarizable Continuum Model.

Electronic transition	TD//B3LYP/6-31+G(d, p)			
	Energy/ eV ^[a]	f ^[b]	Composition ^[c]	CI ^[d]
S0→S1	2.6513 eV nm	0.2725	HOMO -1→ LUMO	0.4533
			HOMO → LUMO	0.5334
S0→S2	2.7606 eV nm	0.3296	HOMO -1 → LUMO	0.5403
			HOMO → LUMO	0.4408
S0→S3	3.2421 eV nm	0.1056	HOMO -2 → LUMO	0.6879
			HOMO -1 → LUMO	0.1514

PCM-DFT optimized coordinates for *meso*-2-ketopyrrolyl BODIPY **1a**

F	-2.97442500	-0.05047800	2.04099400
F	-4.22904900	0.20534100	0.13134100
N	-2.23428600	-1.17516400	0.02409900
N	-2.07065300	1.30760100	0.24501900
N	2.06125800	-0.20249200	0.98092200
H	1.16226200	-0.15721300	1.43990700
O	1.28371000	0.05575600	-2.54643500
C	-0.80830300	1.25348100	-0.35506900
C	-0.96538300	-1.18203100	-0.56524500
C	-0.25739200	0.01784800	-0.72686800
C	-2.70208400	-2.44052900	0.04711100
C	-2.37462800	2.59955900	0.48729200
C	-0.65403000	-2.53316000	-0.92774900
C	2.24482900	-0.14368700	-0.39703200
C	-0.32693800	2.59647700	-0.49336200
C	-1.31497900	3.43295300	0.03731400
C	3.25856500	-0.32184500	1.61285000
C	1.14362900	-0.02013200	-1.32339800
C	4.26264300	-0.34849500	0.63372900
C	3.62766800	-0.23605400	-0.63117300
C	-1.75090600	-3.31312900	-0.54690500
B	-2.92916100	0.07254000	0.63692300
C	-4.03687600	-2.78720000	0.62400800
H	-4.14732800	-2.36807900	1.62871300
H	-4.16562100	-3.86960800	0.67810600
H	-4.84480400	-2.36746400	0.01481200
C	3.35451800	-0.37903400	3.10514000
H	3.51093200	0.61585200	3.54093100
H	4.19273000	-1.00784100	3.41791600

H	2.44275300	-0.79448900	3.54647100
C	-3.65821100	3.00859600	1.13436600
H	-4.50465500	2.82989500	0.46235100
H	-3.63902300	4.06856300	1.39476300
H	-3.84365900	2.42348100	2.03995700
C	0.57843400	-3.02931400	-1.62623700
H	0.70129900	-2.55829700	-2.60662000
H	0.52837300	-4.11066000	-1.77243800
H	1.48780600	-2.81611800	-1.05365500
C	0.95872300	3.04384700	-1.12620800
H	1.83484600	2.62555300	-0.61901900
H	1.04450400	4.13219900	-1.09286700
H	1.01910500	2.73217200	-2.17380000
C	5.74204100	-0.44856800	0.89770900
H	5.91016900	-0.98401000	1.84019900
H	6.21165900	-1.06259900	0.11975200
C	4.29192100	-0.22164900	-1.97579700
H	3.78153200	-0.88591700	-2.67816300
H	5.34009900	-0.52372100	-1.90008400
H	4.26020700	0.77836200	-2.42436000
C	-1.30475800	4.93770400	0.09541600
H	-1.81683300	5.27307500	1.00546900
H	-0.27242400	5.29281400	0.19175600
C	-1.95858000	5.61111200	-1.12698600
H	-3.00677400	5.31066500	-1.22927800
H	-1.44355800	5.33020700	-2.05168300
H	-1.92582200	6.70268600	-1.03618200
C	-1.91288800	-4.80149300	-0.71069300
H	-2.97341700	-5.04204700	-0.84837300
H	-1.41733900	-5.12274000	-1.63411600
C	6.45705300	0.91500800	0.96022400
H	6.04560200	1.53946900	1.76067100
H	6.33967000	1.46361100	0.01986100
H	7.52920400	0.78723400	1.14699400
C	-1.35778500	-5.62075200	0.47083000
H	-1.49927400	-6.69448900	0.30378700
H	-1.85992700	-5.35384300	1.40699900
H	-0.28685100	-5.43591400	0.60718000